Spacetime & Substance

International Physical Journal

Volume 3, No. 5 (15), 2002

EXPERIMENTAL EVIDENCE OF THE MICROWAVE BACKGROUND RADIATION FORMATION THROUGH THE THERMAL RADIATION OF METAGALAXY STARS

V.S. Troitskij, V.I. Aleshin[1]

Radiophysical Research Institute, N.Novgorod, Russia

The paper is devoted to the development of the theory of microwave background formation through the optical radiation of Metagalaxy stars which is transformed due to the redshift into the microwave and infrared star background radiation. An application of the theory to the model of a stationary nonexpanding Universe of a size not less than 40–50 thousand Mpc shows that the star microwave background is not strictly the blackbody one. Its brightness temperature and spectral density correspond to $2.73K$ in Rayleigh-Jeans region of the background $\lambda > 1mm$, but grow significantly in submillimeter,infrared and optical wave ranges. This prediction is confirmed by available measurements up to optical wavelengths. Besides, the value and dependence of small-space background fluctuations on the angular resolution and the wavelength predicted by the theory is in a good agreement with the experimental data. Finally, the fact, mysterious from the background relic origin point of view, of equality of the volume background energy density and the optical star radiation energy has a very simple and natural explanation. An application of the theory to the closed model of the Universe in the big-bang cosmology shows that at wavelengths $\lambda > 1mm$ the star background is negligibly small (no more then 0.1K), but at submillimeter waves it significantly exceeds 2.7K that comes into conflict with the hypothesis of the background relic origin and the idea of the big bang. It follows from the results obtained that the observable nonblackbody electromagnetic background is not a relic one and it has a star origin.

> *For majority opinion to change on the correctness of the hot big-bang cosmology, it is clear that one or more of the arguments given above must be seen to fail ... . However, if a change does occur, it will probably come from one of three directions: ...*
> *b) A demonstration that there is an other plausible mechanism which could be responsible for the MBR, probably related to the idea that it does not have a perfect blackbody spectrum and/or that it could not have been coupled to the matter at an earlier epoch (Burbidge, 1989, p. 988)*

Introduction

The idea to explain the microwave background radiation by sources of different nature is not new, but it has not yet been worked out in any concrete form.

In this paper we investigate a possibility to explain the observed microwave background by the thermal radiation of the Metagalaxy stars. For this purpose it is evident to use some cosmological models of the structure and evolution of the Universe. The problem of the contribution of the star integral radiation in standard cosmology models was studied earlier. First studies in this direction were carried out by McVittie(1962). On the methodical basis of this work Doroshkevich and Novikov(1964) have published only results of colculations for different models of the standard cosmology.

The methods of calculations were not given. It has been shown, in particular, that at a wavelength of observation $\lambda_o > 1mm$ the volume energy density of the star integral radiation is much less than the blackbody radiation with the temperature $T = 1K$. There was an affirmation (Parijskij and Sunyaev 1973) that "the observed relic radiation cannot be explained by the integral radiation of discrete sources" in standard cosmology models. To calculate the radiation of galaxies, as correctly noted by Zel'dovich and Novikov (1967), "is of prime importance in a hot model since it is the background on which the relic radiation of the model itself is to be observed."

This is a valuable but unused so far test of the background relic origin theory. Recently there have been some serious experimental demonstrations that the standard cosmology does not reflect any more a real state of matter and radiation in the Universe (lu-

---

[1] e-mail: redshift0@narod.ru

minosity of galaxies, their dimensions and evolution) (Segal 1992; Troitskij 1992,1994). In this connection and due to existing alternative cosmological theories it becomes important to explain the microwave by other physical reasons, in particular, by the optical radiation of stars in distant galaxies transformed into the radio-frequency band owing to the redshift of the radiation of stars along the path to an observer.

In this formulation the problem requires justified physical procedures of calculation for its solution which are absent in full measure so far. The method of calculation and the first estimations presented earlier (Troitskij 1994) had shown that in a static nonexpanding Universe the 3K background can be explained by the thermal radiation of stars if the size of the stationary Universe is at least by an order more than that of the generally adopted. In this present paper we give a detailed physical justification of the calculation method which is then applied to BGR calculation for different models of the Universe including the standard one. A comparison is made for the results obtained for different models with the observed characteristics of the microwave background. This may a good test to choose this or that theoretical model most adequate with the reality (see reviews of Baryshev 1992, Burbidge 1989). All said above justifies the statement of the present work.

1. Physical basis of star microwave background formation

To determine this radiation let us consider the Universe as the Euclidean space filled with matter in the form of galaxies being the clusters of stars of different spectral classes. We suppose that the spatial distribution of galaxies in the Metagalaxy space is uniform and isotropic and their mean parameters over a sufficiently large volume do not depend practically on the distance. We suggest as well the star thermal radiation as a blackbody one. At first let us consider the solution of the problem in a simplified form taking the temperature of all stars equal in the whole galaxy. Let n gal/Mpc be the mean volume density of galaxies, m, the mean number of stars in the galaxies, r, their mean radius, T, the mean temperature of their photospheres. Let us take into account that the stars in galaxies are not practically projected to which other.

Let us find the spectral power density of the thermal radiation flux from stars at radio frequency ν_0 in the antenna aperture with reception diagram Ω sterad. The full flux from the galaxies at metric distance R in volume element $R^2 \Omega \, dR$ is

$$d\Phi = F(\nu, T) \pi r^2 n \, m \, R^2 \Omega \, dR \, d\nu. \qquad (1)$$

Here ν is the radiation frequency of stars in their own reference frame, $F(\nu, T)$ is the Plank's function

for the spectral density of the star blackbody emissivity $W/cm^2 Hz \, sr$. Along the path of propagation up to a telescope antenna this radiation at frequency ν will have three types of attenuation and a frequency transformation due to the redshift. The first type is the attenuation in R^2 times, the second type is the energy absorption in the propagation medium which we shall describe by the function $\gamma(R)$. And at last the third type of attenuation is connected with the redshift of frequency ν up to observation frequency $\nu_0 = \nu/(z+1)$. To determine this type of attenuation there is no need to use any hypothesis on the redshift nature except the fact of its existence. Let us consider the star radiation with a spectral density $F(\nu T)$ at frequency ν in a narrow frequency band $d\nu$. At the observation point all this spectrum will be seen shifted down with boundary frequencies $\dfrac{\nu - 0.5\Delta\nu}{(z+1)}$ and $\dfrac{\nu + 0.5\Delta\nu}{(z+1)}$ with unchanged spectral density $F(\nu_0 T)$ since its increase in $(z+1)$ times due to the spectrum contraction is compensated in the same times by weakening of the quantum energy from $h\nu$ to $h\nu_0$. Thus, the energy of the shifted spectrum is equal to the integral of $F(\nu T)$ in band $\Delta\nu/(z+1)$ i.e.

$$F(\nu T)\Delta\nu/(z+1) = F(\nu T)\Delta\nu_0,$$

where $\Delta\nu_0 = \Delta\nu/(z+1)$. This result is obtained as well at a purely quantum approach. Indeed, radiation $F(\nu T) \, d\nu$ for very narrow band $d\nu$ is a practically a monochromatic one and its power is proportional to $h\nu$. At the reception point this monochromatic radiation will have energy proportional to $h\nu_0$, i.e. less in $(z+1)$ times as compared with the radiated one. The same extinction will be as well in the case of a wide reception band, overlapping all the spectrum of the observed radiation. To illustrate this point let us find the total energy received from the source with redshift z. As above, we suggest the source radiation in its frame of reference have Planck spectrum. In this case each frequency at the observer of the whole spectrum extending from $\nu = 0$ to $\nu \to \infty$ will have a shift to zero frequency decreasing in $(z+1)$ times. This spectrum take the form

$$d\nu_0 F(\nu_0) = \frac{2\,h}{c^2}\,\nu_0^3(z+1)^3 \times$$

$$\times \left(\exp\frac{h\nu_0(z+1)}{kT} - 1 \right)^{-1} d\nu_0, \; W/cm^2 sr,$$

where $\nu_0 = \nu/(z+1)$ is the frequency in the observer's reference frame. Integrating over all frequencies ν_0 from 0 to ∞ and using the change of variables $h\nu_0(z+1)/kT = x$ we have an analogue of the Stefan-Boltzmann low

$$P = \frac{2\pi k^4 T^4}{h^3 c^2 (z+1)} \int\limits_0^\infty \frac{x^3}{e^x - 1} \, dx = \sigma T^4/(z+1).$$

Thus, as it is expected all the energy received decreases in $(z + 1)$ times.

It should be noted that in the standard cosmology the attenuation of galaxy radiation caused by the redshift due to the Doppler effect is taken to be equal in $(z + 1)^2$ times, i.e. for the Planck radiation spectrum $F(\nu T) d\nu$ the received signal has power

$$F(\nu T) \, d\nu / (z + 1)^2 = F(\nu T) \, d\nu_0 / (z + 1).$$

This attenuation, as suggested, is due both to the decrease of the quantum energy and their number (or in another words the frequency band). It seems that in this way the attenuation is determined twice: first in $(z+1)$ times due to the decrease of the quantum energy (quantum approach), and then again in $(z+1)$ times due to the decrease of the band (classical approach), we consider such an approach to be groundless.

So then, at the reception place we have the following illumination from the considered volume element

$$dE = \pi r^2 \, n \, m \, \gamma(R) \times$$

$$\times F[\nu_0 (z + 1), T] \Omega \, d\nu_0 \, dR, \ W/cm^2 sr, \qquad (2)$$

where $F[\nu_0(z + 1), T] = 2h\nu_0^3(z + 1)^3/c^2 \, [\exp(h\nu_0(z + 1)/kT) - 1] \, W/cm^2 sr \, Hz$. The full illumination in the antenna aperture from all the galaxies in the solid angle of the radiotelescope antenna is

$$E = \pi \, r^2 \, nm \, d\nu_0 \Omega \int\limits_0^\infty F[\nu_0(z + 1), T] \, \gamma(R) \, dR. \qquad (3)$$

If $\gamma(R)$ is such that at some $R = R_{max}$, $\gamma(R_{max}) = 0$, then the upper limit of the integral will be definite and equal to R_{max}. As it is obvious, at the given galaxy distance R its radiation at frequency ν will come in the reception band at the frequency $\nu_0 = \nu/(z + 1)$, if the galaxy redshift is z. In this way to integrate expression (3) it is necessary to use the functional relation between R and ν or, ultimately, between R and z.

Then, substituting dR in (3) for $dR = \frac{dR}{dz} dz$, $\gamma(R)$ for $\gamma(z)$ we obtain finally

$$E = \pi r^2 \, nm \, d\nu_0 \Omega \times$$

$$\times \int\limits_0^{z_m} F[\nu_0(z + 1), T] \, \gamma(z) \, \frac{dR}{dz} dz, \ W/cm^2 sr. \quad (4)$$

In our case it is expedient to characterize the radiation E by the effective temperature T_b which is defined as a temperature of the blackbody radiation with the same spectral power. Comparing (4) with the radiation of a black cavity

$$E = 2h\nu_0^3 \Omega \, d\nu_0/c^2 [\exp(h\nu_0/kT_b) - 1], \ W/cm^2 sr,$$

we obtain the required expression for the background radiation temperature

$$\pi \, r^2 \, nm \, \frac{2h\nu_0^3}{c^2} \int\limits_0^{z_m} \frac{(z + 1)^3 \gamma(R) \frac{dR}{dz} \, dz}{\exp[h\nu_0(z + 1)/kT] - 1} =$$

$$= \frac{2h\nu_0^3}{c^2 [\exp(h\nu_0/kT_b) - 1]}. \qquad (5)$$

The dimension of (5) is equal to $W/cm^2 Hz \, sr$. In dimensionless form designating $\nu_0 = c/\lambda_0$, where λ_0 is in meters, we have

$$\pi \, r^2 \, nm \int\limits_0^{z_m} \frac{(z + 1)^3 \gamma(R) \frac{dR}{dz} \, dz}{\exp hc(z + 1)/kT\lambda_0 - 1} =$$

$$= \left[\exp\left(\frac{hc}{k\lambda_0 T_b} \right) - 1 \right]^{-1}. \qquad (6)$$

Denoting the left part as x we have for the background temperature

$$T_b(\lambda_0) = \frac{hc}{k\lambda_0 \ln[(x + 1)/x]}. \qquad (7)$$

Expression (6) is simplified if, firstly, in the upper integration limit we have the condition $hc(z_m + 1)/\lambda_0 kT \leq 0.1 - 0.2$ and, secondly, at the desired background temperature T_b $hc/\lambda_0 kT_b \leq 0.1 - 0.2$. As it is, taking the first term of the exponential function expansion we obtain from (6)

$$T_b = r^2 \, nm \, T \int\limits_0^{z_m} (z + 1)^2 \gamma(z) \frac{dR}{dz} dz. \qquad (8)$$

At $z_m = 3000$ and $T = 6 \cdot 10^3 \, K$ the first condition is fulfilled for $\lambda_0 \geq 3$ cm and the second one at $T_b \sim 3K$ is fulfilled for $\lambda_0 \geq 2.5$ cm.

Now for integrating it is necessary to know $R(z)$ in the interval $0 \leq z \leq \infty$. For this purpose one can use in the first approximation the Hubble law $R = R_0 \, z$ established experimentally for $z \leq 0.02$ or the law $R = R_0 \sqrt{z}$ verified by the observations of galaxies and quasars in the interval $0 \leq z \leq 5$ (Segal 1993, Troitskij 1994). Then, for calculation it is necessary to determine the attenuation function $\gamma(R)$. This can be done on the basis of different physical grounds. At first we suggest the simplest ones, namely, that beginning from some distance R_m the radiation from sources out from regions $R > R_m$ is completely screened (or absorbed) by the central parts of galaxies lying on the path of wave propagation. This takes place when projections of all central parts of galaxies lying in the sight cone of length R_m are merging and taking area ΩR_m^2. The number of galaxies in cone Ω up to distance R is equal to $N = nR^3\Omega/3$. The total projection area of their central parts of diameter $1 \, kPc$ is $S = 0.25n\Omega R^3 l^2$. This

area covers the part of the cross-section area of cone ΩR^2. Hence, only a part of radiation will pass through the cross-section $\gamma(R) = 1 - 0.25 R n l^2$. The channel will be fully closed when $\gamma = 0$, i.e. at $R_m = 1/0.25 n l^2$, then $\gamma(R) = 1 - R/R_m$ or at $R = R_0 \sqrt{z}$ we have $\gamma(z) = 1 - \sqrt{z/z_m}$. Here the attenuation (or screening) function does not depend on the wavelength that takes place practically for the optical radiation forming the observed background. Let us take for the calculation $l = 6 \, kPc$, $n = 2$, then $R_m \simeq 50000 \, MPc$, $z_m \simeq 6 \, 10^3$.

In the given estimation the galaxies and the stars inside the galaxies are regarded immovable relative the given spherical coordinate system with a centre at the observer. In reality there exist proper motions of the galaxies as well as the stars inside them. It is obvious that the account of these motions does not change the result obtained. Indeed, in a sufficiently large volume, say $\simeq 10^3 MPc$, containing several thousand galaxies the directions of motions are distributed isotropically and the velocity values are distributed according to the normal law with the rms velocity $\sim 300 km/s$. So, the radiation of galaxies will have the frequency shift not more than $\Delta \nu / \nu \simeq \pm v/c \simeq 10^{-3}$. Owing to this fact the observed radiation temperature from each galaxy well differ from the average one not more than $\Delta T/T \leq \pm 10^{-3}$. Due smallness of the effect and its homogeneity when adding radiation of a large number of galaxies, the influence of this chaotic velocities on the radiation frequency and temperature will be mutually compensated. The same can be said on the influence of the velocity dispersion of the galaxy stars. Thus, the uniform and isotropic microwave background fixes in a statistical sense the immovable coordinate system resting on all the galaxies of the visible part of the Universe.

2. Jeneral expression for star microwave background radiation of the Metagalaxy

In this section we give quite a general expression for the star background suitable for different models of the Universe. We suggest space filling with the galaxies be uniform and isotropic and their mean luminosity and dimensions be invariant in time and space. The problem is to give a calculation taking into account a contribution of the stars of different spectral classes, i.e. with different photosphere temperatures and sizes. As it is known, more than 80 per cent of stars in galaxies are those of the main sequence and hence they will determine chiefly the observed star background. For this stars the required parameters r and T are given through the star luminosity M, determining its spectral class, radius and photosphere temperature. Let us use the known formula for the relative stellar radius

$r/r_\odot$

$$\lg r/r_\odot = \frac{5000}{T} - 0.2 M - 0.02, \qquad (9)$$

where T is the photospheric temperature of the star and M is its photographic value. The relation M_T is usually given in tables and for the stars of the main sequence it is approximated with a sufficient accuracy by the function

$$T = \frac{26 \, 10^3}{0.37 \, M + 2.4}. \qquad (10)$$

Substituting (10) into (9) we have

$$\frac{r^2}{r_\odot^2} = 10^{-0.233 M + 1.05}. \qquad (11)$$

The luminosity distribution of the main sequence stars $\varphi(M)$ has been known (see, for example Lang 1974). The luminosity function $\varphi(M)$ is given in the table form in the interval $M \pm \frac{1}{2}$ near the integer value from $M = -4$ to $M = 20$ that involves spectral classes $B \, A \, F \, G \, K \, M$. The intervals of M values of these spectral classes are equal respectively to (-4,-1), (0,+3), (+4,+6), (+7,+9), (+10,+19). We have used normalization $\sum \varphi(M) = 1$. As a result, the full radiation will be

$$\pi \, r_\odot^2 \, n m \sum_{-4}^{19} 10^{-0.233 M + 1.05} \, \varphi(M) \times$$

$$\times \int_0^{z_m} \frac{(z+1)^3 \gamma(z) \frac{dR}{dz} \, dz}{\exp\{hc(z+1)/\lambda_0 kT\} - 1} =$$

$$= \left[\exp \frac{hc}{k \lambda_0 T_b} - 1 \right]^{-1}. \qquad (12)$$

Here T is defined by (10). Function dR/dz is determined by accepted theoretical or experimental dependence $R(z)$. Expression (12) does not depend explicitly on the accepted nature of the redshift. Its nature manifests only through concrete functions $R(z)$. For the experimental model of the Universe $R(z) = R_0 \sqrt{z}$, for the closed model of the standard cosmology $R(z) = cH^{-1} z/(z+1)$ and so on.

3. Star microwave background radiation in a static model of the Universe

We consider the static model of the Universe. Space filling with the galaxies is uniform and isotropic in scales estimated by contemporary observations. We also suggest the mean dimensions and luminosity in the same scales to be invariant in time and in the whole Metagalaxy space. It is essential that this model follows

from observed mean (statistical) dependences of apparent luminosity $\overline{m(z)}$ and angular dimensions $\overline{\theta(z)}$ of the galaxies and quasars which make possible to determine the really existing dependence $R(z)$ equal to $R = 600\sqrt{z}\,\mathrm{Mpc}$ in the redshift interval $0 \leq z \leq 5$ (Troitskij 1995). Taking into account in (12), that $R = R_0\sqrt{z}$, where $R_0 = 600Mpc$ we have

$$A\sum_{-4}^{19} 10^{-0.233M+1.05} \varphi(M) \times$$

$$\times \int_0^{z_m} \frac{z^{-1/2}(z+1)^3\gamma(z)\,dz}{\exp\{hc(z+1)/\lambda_0 kT\} - 1} =$$

$$= \left[\exp\frac{hc}{k\lambda_0 T_b} - 1\right]^{-1}. \quad (13)$$

Here T is given by (10), $A = \frac{1}{2}\pi r_\odot^2\,n\,m\,R_0$.

Parameter A may have only admissible limits of possible values since a strict mean value of nm, i.e. a star number in a cubic Mpc, is unknown. According to the data on the population of the Local Group containing three large galaxies with the star number $m = 10^{11} - 10^{12}$ and about two tens with the star number one-one and a half orders less one can take $10^{10} \leq nm \leq 10^{11}$. Then at $R_0 = 600\,Mpc$ admissible value of A lies in the interval $10^{-12} \leq A \leq 10^{-10}$, which may be used in the background calculation. Then taking the mean size of the central part of galaxies $l \simeq 6\,Kpc$ we have $\gamma(z) = 1 - \sqrt{z/z_m}$, where $z_m \sim 5000 - 7000$.

The calculation results of the background temperature are given in Tables 1 and 2 in the waveband from $1m$ to parts of a micron. The first table has been calculated for the law $R = R_0\sqrt{z}$, the second one for the Hubble linear law $R = R_H z$ extrapolated beyond the limits of its experimental grounding within the interval $0 \leq z \leq 0.02$. The comparison of two tables shows there is not any significant difference in the background temperature dependence on wavelength. It can be seen from the tables that at waves $\lambda > 1mm$ the background is determined by the stars of spectral classes $A\,F\,G$, at $\lambda < 1mm$ by those of classes $B\,A$ and in the ultraviolet by only those of class B. To check these results we made as well the calculation of the background attenuation in $(z+1)^2$ times due to the redshift. In this case the dependencies remain practically unchanged, but the value of A is an order higher than that as an upper limit estimate both for two laws $R = R_0\sqrt{z}$ and the Hubble one.

A most interesting and unexpected result of the theory is the growth of the background temperature in the submillimetre waveband. Any reasonable attempts to eliminate this growth were failed. Finally, it has been understood that the growth aries due to a sharp difference of the star background from the blackbody one at submillimetre and shorter wavelengths. This has
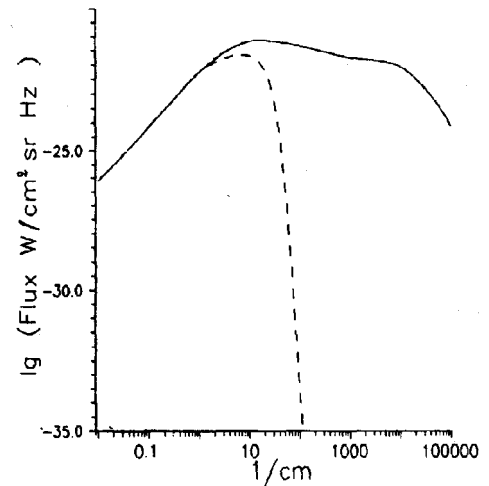
Figure 1: A comparison of the star background spectrum for the universe static model (solid line at $z_m = 5 \cdot 10^3 - 7 \cdot 10^5$) with the blackbody spectrum at $T_b = 2.73K$ (dotted line)

been shown in Fig. 1 where the star background spectrum is given in comparison with the blackbody one at $T = 2.7K$. Theoretical and blackbody spectra at $T = 2.7K$ coincide in the Rayleigh-Jean's region of the Planck's spectrum and sharply differ in the Wiens's region at $\lambda < 1mm$. Here the star spectrum is practically flat and its spectral density exceeds the spectral density of the Planck's spectrum by many orders at $T = 2.7K$ that causes the growth of the equivalent background temperature. The reason of the spectra difference is the fact that the star background is added up basically from the Rayleigh-Jeans's parts of the star radiation spectra which extend to optical frequencies at a high star temperature. Really, the integral in (13)decreases exponentially with the frequency and, hence, beginning with some value of z it does not give any essential contribution in integral (13). One may conclude that this takes place when $hc(z+1)/k\lambda_0 T$ and the expression $hc(z+1)/k\lambda_0 T = 1$ determines at the given values of T and λ_0 an actual upper limit of integration. As a result, each spectral class of stars for different observational waves has its actual upper limit of integration over z related as it is obvious with the cutoff of the star Planck's spectrum in its Wiens's region. Thus, the background radiation is basically made at the star radiation in the Rayleigh-Jeans's region. Table III gives the values of z_{ef}, characterizes the size of galactic layer $R = R_0\sqrt{z_{ef}}$ responsible chiefly for the observed background radiation at a given wavelength. It is seen from the table, that at centimeter and longer waves $\lambda > (0.5 - 1)cm$ the background spectrum intensity is bounded by galaxy screening at $z_m \approx (5 - 7) \cdot 10^3$ and at $\lambda \leq 0.1\,cm$ by the cutoff of the star radiation intensity in the Wiens's spectrum region. As a result,

the background radiation in the Wiens's region is determined by rather a thin layer of galaxies radiations in the Rayleigh-Jeans's region of the spectrum. The reduction in number of galaxies responsible for the background at $\lambda \leq 1mm$ is an important factor which leads to an essential increase of small-scale background fluctuations for shorter waves, that is confirmed by observations.

When calculating the star background we studied how the background temperature is influenced by an increase of the star photosphere temperature at wavelengths longer than 1cm. To estimate this influence we have the only example, the Sun. Its brightness temperature for $\lambda_0 \leq 1m$ may be approximately expressed by the relation $\bar{T} = T_0 + 5 \cdot 10^5 \lambda$, where $\lambda = \lambda_0/(z+1)$ in meters. At such temperature of stars T_b increases at waves $\lambda_0 \geq 20cm$ no more than $0.01K$. At last, as far as, the calculation procedure is concerned, it should be remembered that the background temperature is determined by two values A and z_m. On the basis of above mentioned calculations of the limit visibility z_m was taken as an initial value and a strict value of A is determined from a requirement that at $\lambda_0 = 3cm$ the background temperature should be 2.73K. This value of A is given in tables. It is clear, only those calculations were used where A did not exceed the limits mentioned above.

4. A comparison of predictions of the star background radiation theory with the measurements

Up to now extensive background measurements have been carried up to far IR close to optics. The star background theory may appear to be actual up to optical waves, so the comparison is not to be bound with the submillimetre waveband. Besides, the theory proposed explains naturally the observed small-scale space fluctuations of the background intensity as well as a mysterious so far phenomenon of the equality of the microwave background intensity and the optical radiation of a mean galaxy including ours. These questions are considered in detail below.

4.1. The star background spectrum and observations

Its obvious, that the comparison of the theory with observations is of interest first of all in the submillimetre waveband. The background measurements in this wavelength region have already been in progress for a quarter of a century. They have been started to confirm the blackbody character of radiation at this waves followed from the Big Bang theory. first investigations at wavelengths $\lambda_0 < 1mm$ carried out by three independent laboratories of the USA on the high-altitude balloons and satellite gave contradictory results: some
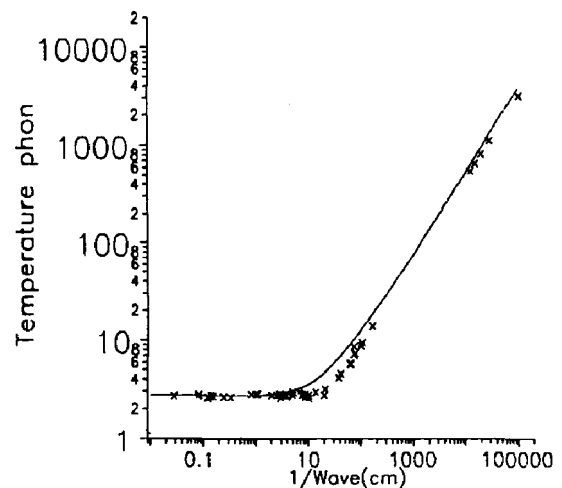
Figure 2: Theoretical dependence of the star background temperature on the wavelength for the static model of the universe at $z_m = (5-7) \cdot 10^3$ as compared with the measurement data (crosses)

got values $T_b = 2.7K$, the others after correction to decrease got $T_b = (3.6-5.5)K$ (see review of Bliter 1974). Note, the measurements giving a higher temperature then $2.7K$ were and are being questioned since they contradict the standard cosmology theory. However, the data mentioned have last their meaning because of uncertainty in the value of the observation wavelength due to a wide band comparable with the mean frequency of reception.

At present there have been reliable results in the work of Matsumoto (1988) at wavelengths 1.16, 0.7, 0.48, 0.137 and 0.1 mm the accuracy of which is not worse than (3-5)%. According to the IRAS (infrared astronomical satellite) program the background measurements have been carried out at 0.1 mm and 0.6 mm, they have been presented in Matsomoto's paper after correction. Most of these results are given in flux units $W/cm^2.sr.Hz$ with exception of data at 1.16, 0.7 and 0.48 mm for which there have been the background brightness temperatures as well. The values of the background temperatures for rest of the waves have been calculated according to relation $B(\nu) = 2h\nu_0^3/c^2(\exp h\nu/kT_b - 1)$, where $B(\nu)$ — is the measured radiation flux in $W/cm^2 srHz$. A test calculation of the temperature for three above mentioned waves have proved the correctness of the temperature calculation by this relation for other fluxes.

Recently the measurements of the cosmic microwave background were carried out by satellite COBE (Cosmic Background Explorer) with a help of receiver FIRAS (Far-Infrared Absolute Spectrometer) in the wavelength band 0.5-5 mm (Mather, et al 1994). The background temperature in this continuous band have been found to be equal to $T_b = 2.726 \pm 0.01K$. The satellite

COBE was also used according to the Program DIRBE (Diffuz Infra Red Background Experiment) to get upper limits of background values in the direction of the south ecliptic pole at wavelengths 240, 143, 100 and 60 μm (Kowada, et al. 1994). There have also been the value of the background upper limit at $\lambda = 154\mu m$. We have used as well the review of the background measurements at radio wavelengths (Kogut, et al. 1988). Finally,to make the picture of the background spectrum full we ventured to use data at $0.3 - 0.8\mu m$ (Leinert, et al. 1995; Lang 1974) and in the ultraviolet at 912 angstrom (Vikhlinin 1995). All this mentioned data have been tabulated in Table IV in units of the spectral flux density and brightness temperature. Fig. 2 gives a comparison of these data with the theoretical expression of the background spectrum and Fig. 3 compares them with the background brightness temperature dependence on the wavelength. As it is seen from figures, the theoretical dependencies are quite well confirmed by the experimental data not only at IR but also in optics and the ultraviolet. This is an absolutely sudden result.Some divergence for $T_b(\lambda)$ can be seen in the submillimetre wavebaund. We think this may be a consequence of a systematic error of the measurements which authors had been experiencing a quite natural subconscious pressure of theoretical prejudices. However, we should note that this divergence is eliminated either by an account of nonblackbodiness of the star radiation in the Wien's region or by an account of intergalactic absorption of optical waves or at last by a small reduction in estimates of a relative number of brightest stars in class B. The value 0.15% given in literature and used by ours may be overestimated due to the observational selection. Finally, it must always be kept in mind that the background measurements at wavelengths shorter than 0.5mm are aggravated by a possible impact of the interplanetary and interstar dust radiation. Some hypotheses given in the literature report that the observed background at $\lambda \leq 0.1mm$ is determined to a great extent by the dust at $T \simeq 20K$ and so on. The uncertainty of corrections of this radiation explains naturally a large spread of the data on fluxes of the cosmic origin. However, despite this fact, one can definitely conclude that the experimental data in a wide wave interval do not confirm the hypothesis of the background relic origin and are in a good agreement with the background star theory.

Recently the background measurements have been made by the population of levels of the hyperfine structure at mm waves in carbon clouds with the redshifts $z = 1.776$ and $z = 2.9$ being near quasars. In the first case the first level of the carbon hyperfine structure has been used and the temperature $T_b(1.7) = 13.5K$ has ben obtained (Songaila, et al. 1994). This result fits formally the Big Bang theory which gives $T_b(z) = 2.73(z + 1)$. However, to explain these experiments we cannot exclude possible energy pumping from a neigh-
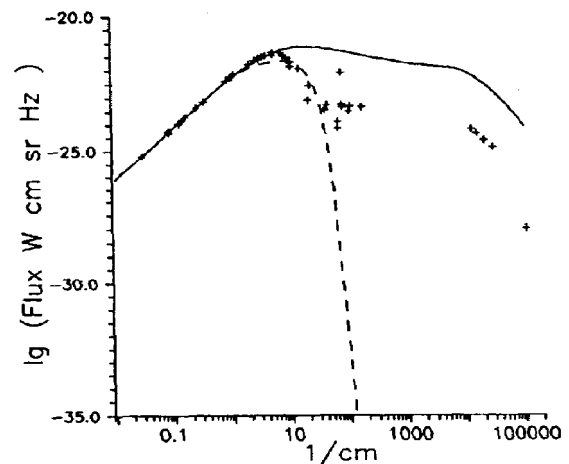
Figure 3: Theoretical spectrum of the star background at $z_m = (5 - 7) \cdot 10^3$ as compared with the measurement data (crosses)

boring quasar (in the first case quasar Q1331+1700), so these data were not included in Table IV.

In conclusion one cannot but note an extraodinary stability of the calculated background spectra to the alterations of the calculation parameters $A, \varphi(M), z_m$ and its dependence on the wavelength $z_m(\lambda)$ and so forth. It even tuned out that the spectrum was not practically changed if we had used a simplified expression (6) for stars of classes FG.

4.2. A mysterious equality of the background energy density and the optical radiation energy of our Galaxy stars has a simple explanation

As it is seen from (2-4) the radiation received by radiotelescopes in a sufficiently narrow band $d\nu_0$ is formed from the radiation of galaxies disposed at different distances R along the line of sight. Each galaxy contributes therewith only at a frequency corresponding to its distance, i.e. $\nu(R) = \nu_0(z + 1)$. No other radiation of the galaxy emitted at other frequencies of its spectrum is received by the radiotelescope tuned at frequency ν_0. If the galaxies have the Planck's radiation spectrum each galaxy contribution is determined by the Planck's function at frequency $\nu(R)$ and is equal to $F[\nu(R), T d\nu_0]$. It is also seen from (2)-(4) that the signal at frequency ν_0 is added up from equal effective number of galaxies for each interval. This takes place obviously because the number of galaxies in each interval R growths as $nR^2\Omega dR$ and their radiation energy at the observer decreases in R^2 times and, hence, is proportional to $n\Omega dR$, i.e. does not depend on distance but only on dR. In doing so we can choose dR in such a way as to have only one galaxy in each interval.

It results that each galaxy in the line of sight would be a lantern of a monochromatic optical radiation of different colors of the Planck's spectrum. However, from the observer's point of view (he is tuned on frequency ν_0) they are one-color radiators at frequency ν_0 placed near the observer. As a result, the contribution of all the galaxies in the radiation received at frequency ν_0 will be equal to the sum of all radiations at all frequencies of the Planck's spectrum from one galaxy. It follows immediately according to (2-6) that the background energy flux is simply equal to the integral over frequency energy flux of the optical radiation of one mean galaxy.

The equality of the blackground energy density and the radiation density of the stars of our Galaxy was discovered more than 15 years ago and was a serious theoretical problem not being solved in the model of the background relic origin. Contrary to this, this fact follows naturally from the theory of the background star origin in a boundness stationary and uniform over all mean parameters Universe. Below we give the corresponding calculations for the volume density of the star background energy.

Expression (5) gives the value of the observed radiation flux spectral density. Multiplying it by $d\nu_0$ and $4/c$ and integrating over frequency ν_0 from zero to infinity we obtain the following expression for the volume density of the background energy

$$\pi\, r^2 n\, m \int\limits_0^\infty \frac{8h\nu_0^3}{c^3} d\nu_0 \int\limits_0^{z_m} \frac{(z+1)^3\, \gamma(z)\, dR}{\exp h\nu_0(z+1)/kT - 1} =$$

$$= \int\limits_0^\infty \frac{8\nu_0^3 h}{c^3}\, \frac{d\nu_0}{\exp h\nu_0/kT_b - 1} = \frac{4}{c}\sigma T_b^4. \quad (14)$$

At $T_b = 2.7K$ the right part gives the radiation volume density $\rho_b = 0.24\,\mathrm{ev/cm}^3$. Now let us calculate the radiation volume density of the stars of our Galaxy. As it is obvious we should take herewith in (14) $z = 0$ and the mean star density nm equal to $m/0.5\, l^3$, where l is a mean diameter of the Galaxy.

$$\rho_* = \frac{2r^2\, m}{l^2} \int\limits_{\nu_0}^\infty \frac{8\pi h\nu_0^3\, d\nu_0}{c^3(\exp h\nu_0/kT - 1)} =$$

$$= \left[\frac{2r^2\, m}{l^2}\, \left(\frac{T^4}{T_b^4} \right) \right] \frac{4}{c}\sigma T_b^4$$

For $t = 6000K$, $l = 15$ kPc, $m = 10^{10}$, $T_b = 2.7K$ the value in square brackets is close to unit and, hence, $\rho_* \simeq \frac{4}{c}\sigma T_b^4 = \rho_b = 0.24\,\mathrm{ev/m}^3$ Thus the approximate equality of the volume densities of the microwave background energy and the optical radiation of our Galaxy is explained by the identity of the nature of the background and the star optical radiation and as well by the
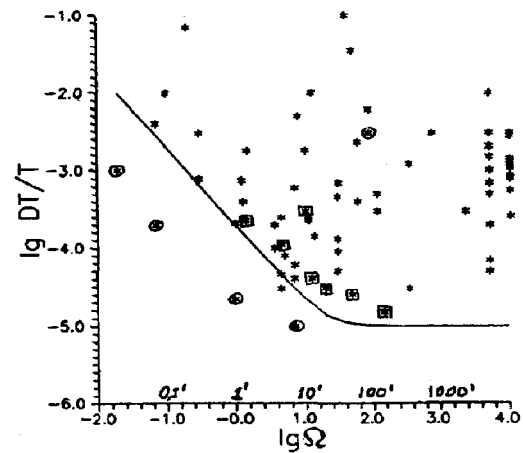
Figure 4: The measurement results of the small-scale space fluctuations of the background temperature $\Delta T/T$ as a function of the radiotelescope antenna pattern width in minutes of arc: ◯ —the measurement of Parijskij; ▫ — the measurements of Berlin. Solid line — the theoretical curve

fact that our Galaxy is close to the mean statistical one. Naturally, this coincidence could not be explained from the point of view of the background relic origin,that was specially noted in the review of Burbidge (1989).

4.3. Background small-scale anisotropy

The spatial variations of the background radiation intensity are determined by a change of $x(\alpha)$ of integral (6) as dependent on direction α of the antenna. In this way according to (7)

$$T_b(\alpha) = hc/k\lambda_0 \ln\left(1 + \frac{1}{x}\right).$$

Usually $x^{-1} >> 1$ and $\Delta T_b/T_b(\alpha) = \Delta x/x$. Then we find a derivative of $\log x$ in (6) and obtain $\Delta x/x = 2\,\Delta r/r + \Delta n/n + \Delta m/m$, here Δr, Δn, Δm are dispersions of corresponding values. The value r is a mean dimension, so $\Delta r \simeq 0$. The dispersion of the number of stars in galaxies , as it is known, is $\sqrt{m}$.

To determine the dispersion of n it is necessary to account the total number of galaxies in the antenna pattern up to the effective distance of visibility $R_e(\lambda) \leq R_m$ depending on λ according to Table III. In the antenna field of sight equal to Ω sterad there will be $N = n\, 0.33\, R(\lambda)^3\, \Omega$ galaxies with dispersion $\Delta N = \sqrt{N} = \sqrt{n\, 0.33\, R(\lambda)^3\Omega}$. Then $\Delta n = \Delta N/0.33 R_e^3(\lambda)\Omega$ and $n = N/0.33 R_e^3(\lambda)\Omega$ from where $\Delta n/n = \Delta N/N = 1/\sqrt{0.33\, n\, R(\lambda)^3\Omega}$. Due to independence of random variables n and m $\Delta T/T = \sqrt{(\Delta n/n)^2 + (\Delta m/m)^2}$

Figure 5: Experimental dependence of $\Delta T/T$ as a function of observation of wavelength

Figure 6: Spatial dependence of the value $X = [(\Delta T/T)^2 - m^{-1}]\Omega$ on the wavelength (solid line) as compared with the experimental data of Table IV (points)

and we have finally

$$\frac{\Delta T}{T} = \frac{1}{\sqrt{m}}\sqrt{1 + m/0.33\, n\, R(\lambda)^3\, \Omega}. \qquad (15)$$
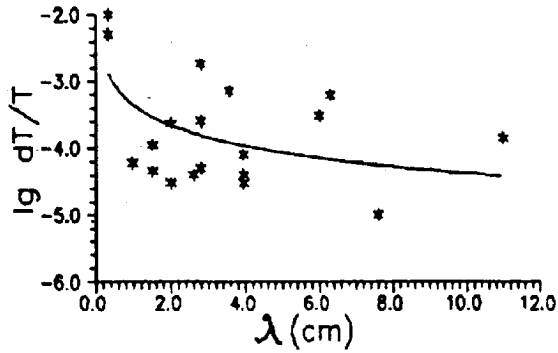
The measurement results of background temperature fluctuations have been given in the review of Parijskij (1990). These results are shown in Fig. 4 in the form of the dependence of $\lg \Delta T/T$ on $\lg \Omega$ in the interval $0 < \Omega \leq 2$, containing 73 data points. The measurement of $\Delta T/T$ were carried out in the wavelength interval $10^{-1} \leq \lambda_0 \leq 50\,\mathrm{cm}$ at a different width of the antenna pattern $0.02' \leq \sqrt{\Omega} \leq 3000'$.

All measurement results are within interval $10^{-5} \leq \Delta T/T \leq 10^{-3}$. It is not possible to reveal any regular behavior in the dependence of $\Delta T/T$ on Ω over all data given in Fig. 4 due to a strong spread of data composed of measurement of different authors and measurement procedures. However, we hope that the data of the same authors for different Ω are most free of relative errors. These data are those of Parijskij and Berlin. According to the data of these authors in Fig. 4 we have clear dependencies of $\Delta T/T$ on Ω. Here as well there has been at he theoretical dependence calculated for $n = 2$, $m = 10^{10}$ and $R_e(\lambda) = 40 \cdot 10^3 Mpc$ valid for $\lambda_0 > 1mm$ which as is seen well agrees with the experimental data of Parijskij and Berlin. Thus, the observed small-scale background anisotropy is explained by discreteness of the background radiation sources, the galaxy stars. Besides, the calculation presented predicts according to (15) and Table III the dependence of $\Delta T/T$ on the observation wave through the change of the size of the galaxy effective layer taking part in the background formation. To reveal this dependence one should exclude the influence of Ω. For this purpose we have sampled the measurement from the data of Fig. 4 in a sufficiently narrow band $0.8 \leq \lg \Omega \leq 1.2$ and then have plotted the dependence $\Delta T/T$ on λ. Fig.

5 presents this dependence which confirms the prediction. The desired dependence was determined as well from all the data. One can obtain easily from (15) the dependence excluding the influence of Ω, namely

$$X = \left[\left(\frac{\Delta T}{T}\right)^2 - \frac{1}{m}\right]\Omega = \frac{m}{0.33\, n\, R^3(\lambda)}.$$

Here $\Delta T/T$ and Ω are the corresponding experimental data from Fig. 4. Fig. 6 gives the experimental dependence of X on λ in comparison with the th theoretical one. The fact of their proper coincidence is a strong argument in favor of the theory of the star background formation.

5. Star microwave background in the standard cosmology model and in the alternative theories

For general formula (12) will do to calculate the background in this case. A specific point for the standard cosmology models is a restriction of the integration limit in (12) up to $z_m < 10$ owing to a limited existence time of the galaxies. In the process of calculation for the closed model we have to take the theoretical expression for the distance-redshift relation $R(z) = cH_0^{-1}z/(z+1)$, where $cH_0^{-1} = R_H$ is the Universe radius. In this case $dR/dz = R_H/(z + 1)^2$ and the general expression (12) has the following form

$$A_H \sum_{-4}^{19} 10^{-0.233\,M + 1.05}\, \varphi(M) \times$$

$$\times \int_0^{10} \frac{(z + 1)\gamma(z)dz}{\exp\{hc(z + 1)/\lambda_0 kT\} - 1} =$$

$$= \left[\exp\frac{hc}{kT_b\lambda_0} - 1\right]^{-1}, \quad (16)$$

where $A_H = \pi r_{\odot}^2 n\, m\, cH_0^{-1}$. Let us take $H_0 = 75$ $km/s\,Mpc$ and $\gamma(z) = 1$.

Table V gives the calculation result at the minimum value of A for two values of $z_m = 5$ and 10 from where it is seen that the star background temperature exceeds $2.7K$ at submillimetre waves and makes its noticeable part at millimetre waves. From that it follows an unambiguous conclusion that the observed microwave background is to be consisted of the sum of star and relic contributions. In other words the relic background has no place at millimetre and especially submillimetre waves. Hence, we have a definite inconsistency of the Big Bang theory to explain the observed microwave background radiation.

From the given calculation it is clear that none of the models with a hot origin can explain the microwave background by the optical radiation of stars. In this case the existence region of the galaxies form is getting too small limited by the interval $z \leq 10$. Here we include the inflation model and the models based on conformal metrics (Hoyle and Narlikar 1972, Troitskij 1987, Petit 1988). The models of a steady-state, i.e. nonexpanding, nonlimited in space and time Universe are in a particular position. We have here the model which explains the redshift by "quantum aging." In this case, as it is known, the quantum energy is supposed to have an exponential attenuation with distance, that gives $R = R_0 \ln(z + 1)$. Here observation background is also explained by the optical radiation of stars. In conclusion we have to note, that microwave background distortions associated with the interaction of relativistic electrons with photons etc. considered in detail by Sel'dovich and Sunyaev (1992) are also valid in the model of the background star origin.

6. Conclusion

All observatiounal imlications of the MBR star origin theory of the stationary nonlimited in space and time Universe are confirmed by all known experimental data. The theoretical background spectrum obtained is confirmed by experimental data in a wide band from decimetric to IR and, probably, even to optical waves. This demonstrates a plausible mechanism of the background formation resulting in a conclusion that MBR is not a perfect blackbody radiation and cannot be coupled to the matter at a earlier epoch. An additional factor of trust is the explanation of a mysterious equality of the MBR energy density and the optical radiation energy density of stars in our Galaxy, as well as the cause of background small-scale anisotropy which predict value and dependence on the antenna pattern width and observation wavelength are confirmed by the measurements. All this is a serious evidence against the idea of Big Bang and in favor of the steady-state Universe hypothesis.

References

[1] Yu.V. Baryshev. "Progress of Science and Technology," *Gravitation and Cosmology*, 4 (1992), (Moscow, in Russian).

[2] A.D. Bliter. IAU Symposium N63: "Conformation of Cosmological Theories with Observational Data," 1974 (USA).

[3] G.R. Burbidge. Int. J. Theor. Phys., **28**, 983 (1989).

[4] A.G. Doroshkevich, I.D. Novikov. DAN USSR, **154**, 809 (1964).

[5] F. Hoyle and J.V. Narlicar. NNRAS, **155**, 305 (1972).

[6] M. Kawada, J.J. Bock, V.V. Hristov et al. Ap. J. **425**, L-89 (1994).

[7] A. Kogut, M. Beksanelli, G. DeAmici et al. Ap.J. **325**, 1 (1988).

[8] K.R. Lang. Astophysical Formulae, New York (1974).

[9] C.H. Leinert, P. Vässanen, K. Lehtenen. Astron. Astroph. Sup. Ser.,**112**, 99 (1995).

[10] J.C. Mather, E.S. Cheng, D.A. Cottengham. Ap. J., **420**, 439 (1994).

[11] T. Matsumoto, H. Hayakawa, H. Matsyo et al. Ap. J. **329**, 567 (1988).

[12] G.C. McVittie. Phys. Rev. **128**, 2871 (1962).

[13] Yu.N.. Parijskij and D.V. Korol'kov. Progress of Science and Technology. Astronomy, **31**, 73 (1986).

[14] Yu.N. Parijskij and R.A. Sunyaev. IAU Symposium N63: "Confrontation of Cosmological Theories with Observational Data," 1974 (USA).

[15] J.P. Petit. Modern Physics Letters A. **3**, 1527 (1988).

[16] E. Segal. Proc. Natl. Acad. Sci. USA **90**, 4798 (1993).

[17] A. Songaila, L. Cowre, C. Hogan, M. Bugers. Nature, **368**, 599 (1994).

[18] A. Songaila et al. Nature, **371**, 43 (1994).

[19] V.S. Troitsky. Ap. Space Sci., **139**, 389 (1987).

[20] V.S. Troitsky. Ap. Space Sci., **201**, 203 (1993).

[21] V.S. Troitskij. Izvestiya Vuzov, Radiofizika, **36**, 857 (1993).

[22] V.S. Troitskij. NIRFI Preprint, N400 (1994).

[23] V.S. Troitskij. UFN, **65**, 703 (1995).

[24] A. Vikhlinin. Pis'ma v A. Zh., **21**, 413 (1995).

[25] Ya.B. Zel'dovich and I.D. Novikov. "Relativistic Astrophysics," Moscow, 1967 (in Russian).

[26] Ya.B. Zel'dovich and R.A. Sunyaev. "Astrophysics and Cosmic Physics," ed Sunyaev R.A., Nauka, Moscow, 1982.

Table I

The star background radiation in the static model of the universe at $R = R_0\, z^{1/2}$ for different combinations of parameters A and z_m. Columns 2-6 are the relative contributions of the stars of spectral classes $B\ A\ F\ G\ K\ M$ into the background radiation. The first line of the columns 2-6 is a relative number of the stars of the given class.

$A = 0.11488E$ - $10\ MAX\ Z = 7000.0$

λ(mm)	B/S	A/S	FG/S	K/S	M/S	T_{back}
	0.013%	1.40%	7.47%	9.29%	81.82%	
0.0001	0.986	0.014	0.000	0.000	0.000	3668.36
0.001	0.219	0.560	0.195	0.023	0.003	520.08
0.010	0.238	0.543	0.189	0.025	0.005	71.95
0.100	0.231	0.547	0.191	0.025	0.005	11.88
1.000	0.165	0.568	0.228	0.032	0.006	3.09
10.000	0.061	0.480	0.358	0.075	0.025	2.56
30.000	0.053	0.454	0.373	0.086	0.034	2.73
100.000	0.050	0.445	0.378	0.090	0.037	2.81
200.000	0.050	0.443	0.379	0.090	0.038	2.83
400.000	0.050	0.442	0.379	0.091	0.039	2.84
800.000	0.049	0.442	0.379	0.091	0.039	2.85
700.000	0.049	0.442	0.379	0.091	0.039	2.85
1000.000	0.049	0.441	0.379	0.091	0.039	2.85

$A = 0.25633E$ -$10\ MAX\ Z = 5000.0$

λ(mm)	B/S	A/S	FG/S	K/S	M/S	T_{back}
	0.013%	1.40%	7.47%	9.29%	81.82%	
0.0001	0.986	0.014	0.000	0.000	0.000	3740.04
0.001	0.220	0.560	0.193	0.023	0.003	535.29
0.010	0.237	0.543	0.190	0.025	0.005	74.92
0.100	0.228	0.549	0.193	0.026	0.005	12.68
1.000	0.141	0.570	0.245	0.036	0.007	3.53
10.000	0.057	0.469	0.365	0.080	0.028	2.72
30.000	0.052	0.450	0.375	0.087	0.035	2.73
100.000	0.050	0.444	0.378	0.090	0.038	2.74
200.000	0.050	0.442	0.379	0.091	0.038	2.74
400.000	0.049	0.442	0.379	0.091	0.039	2.74
800.000	0.049	0.441	0.379	0.091	0.039	2.75
700.000	0.049	0.441	0.379	0.091	0.039	2.75
1000.000	0.049	0.441	0.379	0.091	0.039	2.75

$A = 0.88421E$ - $10\ MAX\ Z = 3000.0$

λ(mm)	B/S	A/S	FG/S	K/S	M/S	T_{back}
	0.013%	1.40%	7.47%	9.29%	81.82%	
0.0001	0.986	0.014	0.000	0.000	0.000	3857.52
0.001	0.222	0.561	0.191	0.023	0.003	560.66
0.010	0.235	0.544	0.191	0.025	0.005	80.00
0.100	0.220	0.551	0.197	0.026	0.005	14.13
1.000	0.108	0.558	0.281	0.044	0.010	4.31
10.000	0.054	0.458	0.371	0.084	0.032	2.89
30.000	0.051	0.447	0.377	0.089	0.037	2.73
100.000	0.050	0.443	0.379	0.090	0.038	2.67
200.000	0.050	0.442	0.379	0.091	0.039	2.66
400.000	0.049	0.441	0.379	0.091	0.039	2.65
800.000	0.049	0.441	0.379	0.091	0.039	2.65
700.000	0.049	0.441	0.379	0.091	0.039	2.65
1000.000	0.049	0.441	0.380	0.091	0.039	2.65

Table II

The same as in Table I, but for the Hubble law R=R$_H$ * z.

A = 0.11362E - 11 MAX Z=3000.0

λ(mm)	B/S	A/S	FG/S	K/S	M/S	T_{back}
	0.013%	1.40%	7.47%	9.29%	81.82%	
0.0001	0.994	0.006	0.000	0.000	0.000	3381.34
0.001	0.350	0.517	0.121	0.011	0.001	488.63
0.010	0.313	0.520	0.147	0.017	0.003	71.29
0.100	0.285	0.535	0.159	0.019	0.003	12.82
1.000	0.119	0.573	0.263	0.038	0.007	4.09
10.000	0.055	0.460	0.370	0.084	0.032	2.86
30.000	0.051	0.447	0.377	0.089	0.037	2.73
100.000	0.050	0.443	0.379	0.090	0.038	2.68
200.000	0.050	0.442	0.379	0.091	0.039	2.67
400.000	0.049	0.441	0.379	0.091	0.039	2.66
800.000	0.049	0.441	0.379	0.091	0.039	2.66
700.000	0.049	0.441	0.379	0.091	0.039	2.66
100.000	0.049	0.441	0.380	0.091	0.039	2.66

A = 0.25601E - 11 MAX 2=5000.0

λ(mm)	B/S	A/S	FG/S	K/S	M/S	T_{back}
	0.013%	1.40%	7.47%	9.29%	81.82%	
0.0001	0.994	0.006	0.000	0.000	0.000	3264.10
0.001	0.351	0.516	0.120	0.011	0.001	465.14
0.010	0.315	0.519	0.146	0.017	0.003	66.45
0.100	0.296	0.529	0.154	0.018	0.003	11.40
1.000	0.166	0.582	0.218	0.029	0.005	3.28
10.000	0.058	0.472	0.364	0.079	0.028	2.68
30.000	0.052	0.451	0.375	0.087	0.035	2.73
100.000	0.050	0.444	0.378	0.090	0.038	2.76
200.000	0.050	0.443	0.379	0.090	0.038	2.76
400.000	0.050	0.442	0.379	0.091	0.039	2.77
800.000	0.049	0.441	0.379	0.091	0.039	2.77
700.000	0.049	0.441	0.379	0.091	0.039	2.77
1000.000	0.049	0.441	0.379	0.091	0.039	2.77

Table III

The dependence of the effective distance of different spectral class on the observation wavelength.

λ_0 cm	$T = 25 \cdot 10^3$ Z_e	$T = 10 \cdot 10^3$ Z_e	$T = 6 \cdot 10^3$ Z_e	$T = 4 \cdot 10^3$ Z_e
10	$175 \cdot 10^3$	$70 \cdot 10^3$	$42 \cdot 10^3$	$28 \cdot 10^3$
1	$17.5 \cdot 10^3$	$7 \cdot 10^3$	$4.2 \cdot 10^3$	$2.8 \cdot 10^3$
0.1	1750	700	420	280
0.01	175	70	42	28
0.001	17.5	7	4.2	2.8
0.0001	1.75	0.7	0.42	0.28

<div align="right">**Table IV**</div>

Experimental measurement data of the background radiation spectral density and its brightness temperature as dependent on wavelength. 1-16 - Kogut 1988, 17-18 - Meyer 1986, 19-24 - Matsumoto 1988, 25-36 - Mather 1994, 37-43 - Kawada 1994, 44-46 - Leinert 1995, 47 - Lang 1974, 48 -Vikhlinin 1995.

No	λ [mm]	$B(\lambda)\cdot 10^{-24}$ W $\text{cm}^2\cdot\text{sr}\cdot\text{Hz}$	T_b [$^\circ K$]	No	λ [mm]	$B(\lambda)\cdot 10^{-24}$ W $\text{cm}^2\cdot\text{sr}\cdot\text{Hz}$	T_b [$^\circ K$]
1	120.000	0.522	2.780	25	350.000	0.060	2.700
2	81.000	1.049	2.580	26	125.000	0.467	2.700
3	63.000	1.801	2.700	27	80.000	1.105	2.650
4	30.000	7.297	2.610	28	70.000	1.465	2.700
5	12.000	42.655	2.780	29	40.000	4.254	2.640
6	9.090	69.962	2.810	30	10.000	59.173	2.800
7	3.330	252.266	2.600	31	5.000	169.739	2.726
8	2.640	331.158	2.700	32	4.000	226.599	2.726
9	2.640	342.627	2.740	33	3.000	306.290	2.726
10	1.320	340.065	2.760	34	2.000	382.538	2.726
11	1.320	335.124	2.750	35	1.000	204.305	2.726
12	3.510	276.694	2.800	36	0.500	8.321	2.726
13	1.980	477.012	2.950	37	0.240	5.600	7.013
14	1.480	456.029	2.920	38	0.154	1.330	5.867
15	1.140	231.624	2.650	39	0.134	5.800	7.221
16	1.000	141.735	2.550	40	0.130	4.800	7.305
17	2.640	339.750	2.730	41	0.100	3.300	8.820
18	1.320	360.202	2.800	42	0.095	5.000	9.436
19	1.160	302.769	2.790	43	0.060	4.800	13.726
20	0.709	116.866	2.956	44	0.0008	0.650	554.560
21	0.481	29.404	3.179	45	0.00035	0.135	1126.722
22	0.262	3.678	4.125	46	0.0005	0.250	826.945
23	0.137	82.966	8.650	47	0.00065	0.450	662.294
24	0.102	3.700	8.740	48	0.00000912	0.0001	3181.021

<div align="right">**Table V**</div>

The star component of the background for the closed model of the universe in the standard cosmology.

<div align="center">A = 0.15000 *E*-11 *MAX* Z = 10.0</div>

λ(mm)	B/S	A/S	FG/S	K/S	M/S	T_{back}
	0.013%	1.40%	7.47%	9.29%	81.82%	
0.001	0.121	0.579	0.260	0.035	0.005	469.81
0.010	0.057	0.466	0.366	0.081	0.030	54.08
0.100	0.050	0.444	0.378	0.090	0.038	5.98
0.500	0.049	0.442	0.379	0.091	0.039	1.28
1.000	0.049	0.441	0.380	0.091	0.039	0.66
2.000	0.049	0.441	0.380	0.091	0.039	0.34
4.000	0.049	0.441	0.380	0.091	0.039	0.18
8.000	0.049	0.440	0.380	0.092	0.039	0.09
30.000	0.048	0.437	0.381	0.093	0.041	0.03
100.000	0.046	0.430	0.385	0.096	0.044	0.01
500.000	0.039	0.402	0.397	0.107	0.055	0.00
1000.000	0.034	0.385	0.405	0.114	0.062	0.00

A = 0.15000 *E*-12 *MAX* Z = 10.0

λ(mm)	B/S	A/S	FG/S	K/S	M/S	T_{back}
	0.013%	1.40%	7.47%	9.29%	81.82%	
0.001	0.121	0.579	0.260	0.035	0.005	437.20
0.010	0.057	0.466	0.366	0.081	0.030	49.80
0.100	0.050	0.444	0.378	0.090	0.038	5.46
0.500	0.049	0.442	0.379	0.091	0.039	1.16
1.000	0.049	0.441	0.380	0.091	0.039	0.60
2.000	0.049	0.441	0.380	0.091	0.039	0.31
4.000	0.049	0.441	0.380	0.091	0.039	0.16
8.000	0.049	0.440	0.380	0.092	0.039	0.08
30.000	0.048	0.437	0.381	0.093	0.041	0.02
100.000	0.046	0.430	0.385	0.096	0.044	0.01
500.000	0.039	0.402	0.397	0.107	0.055	0.00
1000.000	0.034	0.385	0.405	0.114	0.062	0.00

A = 0.15000 *E* - 12 *MAX* Z=5.0

λ(mm)	B/S	A/S	FG/S	K/S	M/S	T_{back}
	0.013%	1.40%	7.47%	9.29%	81.82%	
0.001	0.116	0.578	0.265	0.036	0.005	436.06
0.010	0.055	0.460	0.370	0.083	0.032	49.35
0.100	0.050	0.443	0.379	0.090	0.038	5.39
0.500	0.049	0.441	0.379	0.091	0.039	1.15
1.000	0.049	0.441	0.380	0.091	0.039	0.59
2.000	0.049	0.441	0.380	0.091	0.039	0.30
4.000	0.049	0.440	0.380	0.091	0.039	0.16
8.000	0.049	0.439	0.380	0.092	0.040	0.08
30.000	0.048	0.434	0.383	0.094	0.042	0.02
100.000	0.044	0.422	0.388	0.099	0.047	0.01
500.000	0.035	0.387	0.404	0.113	0.061	0.00
1000.000	0.031	0.372	0.411	0.119	0.067	0.00

THE MEASURING OF ETHER-DRIFT VELOCITY AND KINEMATIC ETHER VISCOSITY WITHIN OPTICAL WAVES BAND

Yu.M. Galaev[1]

The Institute of Radiophysics and Electronics of NSA in Ukraine,
  12 Ac. Proskury St., Kharkov, 61085 Ukraine

The experimental hypothesis verification of the ether existence in nature, i.e. the material medium, responsible for electromagnetic waves propagation has been performed. The optical measuring method of the ether movement velocity and the ether kinematic viscosity has been proposed and realized. The results of systematic measurements do not contradict the original hypothesis statements and can be considered as experimental imagination confirmation of the ether existence in nature, as the material medium.

The experimental hypothesis verification of the ether existence in nature, i.e. material medium, responsible for electromagnetic waves propagation has been performed earlier in the works [1-3], within millimeter radio waves band, by the phase method. The results of the experiment [1-3] do not contradict the original hypothesis statements, based on the ether model of V.A. Atsukovsky [4-6]. In the model [4-6] the ether is introduced by the material medium composed of separate particles, that fills in the world space, has the properties of viscous and coercible gas, is the construction material for all material formations. The physical fields represent the ether various movement forms, i.e. the ether is the material medium, responsible for electromagnetic waves propagation. The experimental model basis [4-6] was, first of all, the positive results of the ether drift search published by D.C. Miller in 1922-1926 [7-9] and A.A. Michelson, F.G. Pease and F. Pearson in 1929 [10].

The experiment [7-9] is performed within the electromagnetic waves optical band, differed by careful preparation, verified methods of the investigation conducting and statistically significant measurement results. The measured ether drift parameters mismatched to the ether imaginations available at that time, as stationary medium. Orbital component of the ether drift velocity, stipulated by the Earth movement around the Sun with the velocity 30 km/sec, was not detected. Miller obtained, that the ether drift velocity at the height of 265 m above the sea level (Clevelend, USA) has the value about 3 km/sec, and at the height of 1830 m (Mount Wilson observatory, USA) — about 10

[1] e-mail: galaev@ire.kharkov.ua; Ph.: +38 (0572) 27-30-52

km/sec. The apex coordinates the Solar system movement were determined: direct ascension $\alpha \approx 17.5^h$, declination $\delta \approx +65°$. Such movement is almost perpendicular to an ecliptic plain (coordinates of the North Pole ecliptic: $\alpha \approx 18^h$, $\delta \approx +66°$). Miller showed, that the observed effects can be explained, if to accept, that the ether stream has a galactic (space) origin and the velocity more than 200 km/sec. Almost perpendicularly directional orbital component of the velocity is lost on this background. Miller referred the velocity decrease of the ether drift from 200 km/sec up to 10 km/sec to unknown reasons.

Some peculiarities of the experiment results [7-9] and [10], are explained by the ether viscosity in the works [4-6]. In this case the boundary layer, in which the ether movement velocity (the ether drift) increases with the height growth above the Earth's surface, is formed at the relative movement of the solar System and the ether near the Earth's surface.

In the works [1-3] it is shown, that the results of systematic experimental investigations within radio waves band can be explained by the wave propagation phenomenon in the moving medium of a space origin with a vertical velocity gradient in this medium stream near the Earth's surface. The gradient layer availability can be explained by this medium viscosity, i.e. the feature proper to material media, the media composed of separate particles. The mean value of the measured maximal gradients was equal to 8.6 m/sec· m. The velocity comparison of the suspected ether drift, measured in the experiments [1-3], [7-9] and [10], is performed in the works [1-3]. The place distinctions of geographic latitudes and their heights above the sea level are taken

into account in these experiments conducting at comparison. It is obtained, that in the experiment [1-3] the ether drift velocity is within $6124\ldots8490$ m/sec, that according to the value order coincide with the data of the works [7-9] and [10], which are within $6000\ldots10000$ m/sec. The comparison result can be considered as mutual truthfulness confirmation of the experiments [1-3], [7-9] and [10].

The positive results of three experiments [1-3], [7-9], [10] give the basis to consider the effects detected in these experiments, as medium movement developments, responsible for electromagnetic waves propagation. Such medium was called as the ether [11] at the times of Maxwell, Michelson and earlier. The conclusion was made in the works [1-3], that the measurement results within millimeter radio waves band can be considered as the experimental hypothesis confirmation of the material medium existence in nature such as the ether. Further discussions of the experiment results [1-3] have shown the expediency of additional experimental analysis of the ether drift problem in an optical wave band.

Experiments [7-9] and [10] are performed with optical interferometers manufactured according to the cruciform Michelson's schema [12,13]. The work of such interferometer based on the light passing in a forward direction and returning it to the observing point along the same path. The Michelson's interferometer sensitivity was low to the original ether drift effects. The measured value D in such a device, i.e. visually observed bands offset of an interference pattern expressed in terms of a visible bandwidth, is proportional to velocity ratio quadrate of the ether drift W to the light velocity c, the optical length of the light beam l and is inversely proportional to the wave length of electromagnetic emission (light) λ [12].

$$D = (l/\lambda)\,(W/c)^2 . \qquad (1)$$

We shall call the interval, which a beam passes in the interferometer measuring part, as the optical length of the light beam. The research methods and experiments in the investigations of the ether drift, in which the measured value is proportional $(W/c)^2$ was called as the "methods and experiments of the second order". Accordingly the methods and experiments, in which the measured value is proportional to the first ratio extent W/c are called as the methods and experiments of the first order. The ratio is $W/c \ll 1$ at the expected value in the experiments of Michelson, Miller $W \approx 30$ km/sec. The methods of the second order are ineffective at this requirement. So at $W \approx 30$ km/sec the method of the second order in 10000 (!) times succumbs on sensitivity to the method of the first order. However at that time the methods of the first order, suitable for the ether drift velocity measuring, were not known.

The expression (1) allows to estimate the difficulties, with which the explorers of the ether drift confronted

in the first attempts while observing the effects of the second order. So in the widely known first experiment of Michelson 1881 [12], at the suspected velocity value of the ether drift $W \approx 30$ km/sec, with the interferometer having parameters: $\lambda \approx 6 \cdot 10^{-7}$ m; $l \approx 2.4$ m, it was expected to observe the value $D \approx 0.04$ of the band. And it is in the requirements of considerable band shivering of an interference pattern. In the work [12] Michelson marked: *"The band were very indistinct and they were difficult for measuring in customary conditions, the device was so sensitive, that even the steps on the sidewalk in a hundred meters from the observatory caused the complete bands vanishing!"*. Later, in 1887, Michelson, also in his world-known work [14], together with E.V.Morly, once again marked the essential deficiencies of his first experiment as for the ether drift [12]: *"In the first experiment one of the basic considered difficulties consisted in the apparatus rotating without the distorting depositing, the second — in its exclusive sensitivity to vibrations. The last was so great, that it was impossible to see interference bands, except short intervals at the business-time in the city, even at 2 a.m. At last, as it was marked earlier, the value, which should be measured, i.e. the interference bands offset because of something on the interval, smaller, than 1/20 of the interval between them, is too small, to determine it, moreover at laying inaccuracies of the experiment"*.

In Miller's interferometer, for sensitivity increase, the optical path length in each of shoulders reached up to 64 meters [7-9]. It was gained due to applying of multiple reflection. The actual length of shoulders was reduced up to 4 meters. In the experiment [10] the optical length of the path reached 26 meters. In the experiments [7-9] and [10] the interferometers laid on rafts, placed in tanks with quicksilver, that allowed to remove the influence of exterior mechanical clutters.

The positive results of Miller's experiment by virtue of their general physical significance attracted the physicists' great attention at that time. In the monographs [15] 150, devoted to the ether drift's problem and referring to 1921-1930, are mentioned that almost everyone were concentrated on the discussion of Miller's results. The possible influencing of the difficult considered exterior reasons (temperature, pressure, solar radiation, air streams etc.) on the optical cruciform interferometer, sensitive to them, which had considerable overall dimensions [16] in Miller's experiments was discussed most widely in these works. Besides by virtue of methodical limitations being in the works [7-9] and [10], their authors did not manage to show experimentally correctly, that the movement, detected in their experiments, can be explained by the Earth relative movement and the medium of material origin, responsible for electromagnetic waves propagation [1-3]. However the most essential reason, which made Miller's contemporaries consider his experiments erratic, was that in numerous consequent works, for example, such as

[17-20], Miller's results were not confirmed. In the experiments [17-20] so-called the "zero results" were obtained, i.e. the ether drift was not detected.

Thus, taking into consideration the works deficiencies [7-9], [10] and a major number of experiments with a zero result available, it is possible to understand the physicists' mistrust to the works [7-9], [10] at that time, the results of which pointed the necessity of the fundamental physical concept variations. The analytical review of the most significant experiments, performed with the purpose of the ether drift search, is explained in the works [1-3, 21].

In 1933 D.K. Miller, in his summary work [22], performed the comparative analysis of multiple unsuccessful attempts of his followers to detect the ether drift experimentally. He paid attention that in all such attempts, except the experiment [10], optical interferometers were placed in hermetic metallic chambers. The authors of these experiments tried to guard the devices from exposures with such chambers. In the experiment [10] it was placed into a fundamental building of the optical workshop at the Mount Wilson observatory for stabilizing the interferometer temperature schedule. The hermetic metallic chamber was not applied, and the ether drift was detected. Its velocity had the value $W \approx 6000$ m/sec. Miller made the conclusion: *"Massive non-transparent shields available are undesirable while exploring the problem of ether capturing. The experiment should be made in such a way that there were no shields between free ether and light way in the interferometer".*

Later, new opportunities for conducting experiments on the ether drift discovery have appeared also after the instruments occurrence based on completely diverse ideas (resonators, masers, Messbauer's effect etc.). Such experiments were held [23-26]. And again the massive metallic chamber usage was the common instrumental error of these experiments. In the works [23,24,26] there were the metallic resonators, in the work [25] — a lead chamber, because it was necessary to use gamma radiation. The authors of these works, perhaps, didn't pay attention to Miller's conclusions of 1933 about the bulk shields inapplicability in the ether drift experiments. The phenomena physical interpretation of the essential ether drift velocity reduction at metallic shields available was given by V.A. Atsukovsky for the first time, having explained major ether-dynamical metal resistance of a Fermi's surface available in them [6].

The purpose of the work is the experimental hypothesis test of the ether existence in nature within an optical electromagnetic waves band — material medium, responsible for electromagnetic waves propagation. It is necessary to solve the following problems for reaching this purpose. To take into account the deficiencies that occurred in the experiments earlier conducted. To elaborate and apply an optical measuring method and

the metering device, which does not iterate the Michelson's schema, but being its analog in the sense of result interpretation. (Michelson's interferometer of the second order is a bit sensitive to the ether streams and too sensitive to exposures.) To execute systematic measurements in the epoch of the year corresponding to the epoch of the experiments implementation [1-3], [7-9], [10]. (The term "epoch" is borrowed from astronomy, in which the observation of different years performed in the months of the same name, refer to the observations of one epoch.) The results of systematic measurements should be compared to the results of the previous experiments. The positive result of the experiment can be considered as experimental hypothesis confirmation of the ether existence in nature as material medium.

Measuring method. The ether model, proposed in the works [4-6], was accepted at making the experiment. The following effects should be observed experimentally within the original hypothesis:

The anisotropy effect — the velocity of electromagnetic waves propagation depends on radiation direction, that is stipulated by the relative movement of the solar System and the ether - the medium, responsible for electromagnetic waves propagation.

The height effect — the velocity of wave propagation depends on the height above the Earth's surface, that is stipulated by the Earth's surface interaction with the viscous ether stream - material medium, responsible for electromagnetic waves propagation.

The space effect — the velocity of wave propagation changes its value with a period per one stellar day, that is stipulated by a space (galactic) origin of the ether drift — the medium, responsible for electromagnetic waves propagation. Thus the height (astronomical coordinate) of the Solar system movement apex will change its value with the period per one stellar day as well as for any star owing to the Earth's daily rotating. Therefore the velocity horizontal component of the ether drift and, hence, the velocity of electromagnetic wave propagation along the Earth's surface will change the values with the same period.

The hydroaerodynamic effect — the velocity of electromagnetic waves propagation depends on movement parameters of viscous gas-like ether in directing systems (for example, in tubes), that is stipulated by solids interaction with the ether stream — material medium, responsible for electromagnetic waves propagation. (As it is known, the law of fluids and gases motions and their interaction with solids is learnt by hydroaerodynamics. This effect, apparently, should be called as the *etherdynamics* effect with reference to the ether dynamics. It can be seen, that "the height effect" is referred to the etherdynamic effect class. However in the work, by virtue of methodical reception distinction used for their discovery, the effects are indicated as separate).

According to the investigation purpose, the measuring method should be sensitive to these effects.

The following model statements are used at measuring method development [4-6]: the ether is a material medium, responsible for electromagnetic waves propagation; the ether has properties of viscous gas; the metals have major etherdynamic resistance. The imagination of the hydroaerodynamic (etherdynamic) effect existence is accepted as the initial position. The method of the first order based on known regularities of viscous gas movement in tubes [27-28] has been proposed and realized within the optical electromagnetic waves band in the work for measuring of the ether drift velocity and ether kinematic viscosity.

The method essence is in the following. Let's place a tube part into a gas stream in such a way, that the direct tube axis will be perpendicular to the stream velocity vector. In this case both opened tube ends in relation to an exterior gas stream are in identical conditions. The gas pressure drop does not occur on the tube part, and the gas inside a tube will be immobile. Then we shall turn a tube in such a way, that the velocity vector of a gas stream will be directed along the tube axis. In this case the gas speedy stream will create a pressure drop on the tube ends, under action of which there is a gas stream in a tube soon. The stabilization time of a gas stream in a tube and this stream velocity are determined by the values of gas kinematic viscosity, the geometrical tube sizes and the velocity of an exterior gas stream [27-28]. Let's mark, that the development of constant gas stream in a tube lasts a terminating interval of time. The ether is a gas-like material medium, responsible for electromagnetic waves propagation according to the accepted hypothesis. It means, that the electromagnetic wave velocity regarding to the observer is the sum of wave velocity vectors relative to the ether and the ether velocity with regard to the observer. In this case, if an optical interferometer is created, in which a beam drives inside a metallic tube, and another outside of a tube (in the ether exterior stream) and to turn the interferometer in the ether drift stream, it can be expected, that in such interferometer, during a stabilization time of the ether stream in a tube, the bands offset of the interference pattern regarding to the original position of these bands on the interferometer scale should be observed. Thus the value of bands offset will be proportional to the ether exterior stream velocity, and the stabilization time — the bands return time to the original position, will be defined by the ether kinematic viscosity value. Hence, the proposed measuring method enables to meter the ether drift velocity values and the ether kinematic viscosity. The proposed measuring method is a method of the first order, as it is not required to revert a light beam to the initial point (as, for example, in Michelson's interferometer).

Let's calculate the interferometer parameters. For the stream analysis of the gas-like ether we shall use the mathematical hydrodynamics apparatus, which is advanced in the works [27-28] at the problem solving,

connected with the stream of viscous incompressible fluid. The use of such solutions for gas stream analysis is true, if the following requirement is performed

$$0.5Ma^2 << 1, \tag{2}$$

where $Ma = w_{pa}c_s^{-1}$ is a Mach's number; w_{pa} is an average gas stream velocity on a tube section; c_s is the gas sound velocity. At the requirement implementation (2), it is possible to neglect the gas pressure effects and consider the gas stream as the stream of incompressible fluid. On data of the experimental works [1-3], [7-9] and [10], the ether drift velocity W near the Earth's surface does not exceed the value $W \approx 10^4$ m/sec. In the work [6] the sound velocity in the ether is estimated by the value $c_s \approx 10^{21}$ m/sec, that essentially exceeds the light velocity. Even if to consider, that $c_s = c$, we shall receive, that $Ma \approx 3.3 \cdot 10^{-5}$. Hence, the requirement (2) is performed, the stream of a gas-like ether can be considered as a stream of viscous incompressible fluid and the use of the hydrodynamics corresponding mathematical apparatus is true for ether stream analysis.

Laminar and turbulent fluid streams are distinguished in hydrodynamics. The laminar fluid stream exists, if the Reynolds number Re, drawn up for a stream, does not exceed some extreme value Re_c [27-28]

$$Re < Re_c. \tag{3}$$

The Reynolds number for a round cylindrical tube is defined by the following expression

$$Re = 2a_p w_{pa} \nu^{-1}, \tag{4}$$

where a_p is the interior tube radius; $v = \mu\rho^{-1}$ is kinematic fluid viscosity; μ is the dynamic viscosity; ρ is the fluid density. Depending on the exterior stream nature and the requirements of fluid influx into a tube, the values Re_c are within $Re_c \approx 2.3 \cdot 10^3 \ldots 10^4$. At $Re < 2.3 \cdot 10^3$ the fluid stream in a tube exists only as laminar and does not depend on an extent of an exterior stream turbulence. The following features are peculiar for a steady laminar fluid stream in a round cylindrical tube. The particle movement pathways are rectilinear. The maximal fluid stream velocity w_{pmax} takes place along the tube axis and is equal to

$$w_{pmax} = 0.25\Delta p a_p^2 \mu^{-1} l_p^{-1}, \tag{5}$$

where Δp is the pressure drop on a tube part with the length l_p;

$$\Delta p = 0,25\gamma_p l_p a_p^{-1} \rho w_{pa}^2; \tag{6}$$

γ_p is the coefficient of a round tube resistance, which is equal $\gamma_p = 64Re^{-1}$ at a laminar regime of fluid stream. The maximal stream velocity w_{pmax} is twice more than mean fluid velocity
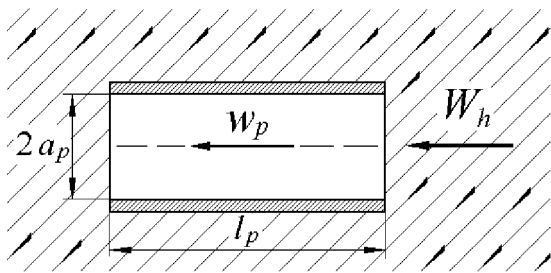
$$w_{pmax} = 2w_{pa}. \tag{7}$$

Figure 1: A tube in a gas stream

The stream velocity distribution on a tube section is called as Puazeyl's parabola and looks like

$$w_p\left(r\right) = w_{pmax}\left(1 - r^2 a_p^{-2}\right),\qquad(8)$$

where r is the coordinate along the tube radius.

The laminar stream transferring into a turbulent one takes place not fluently, but by jumps. At transferring through the extreme value of a Reynold's number the tube resistance coefficient increases by jump, and then slowly reduces. The following features are peculiar for a steady stream of viscous liquid in a round cylindrical tube of turbulent stream. The pathways of particle movement have scattered nature. The resistance coefficient of a round tube is equal $\gamma_p = 0.3164 Re^{-0.25}$. The velocity distribution on a tube section is almost uniform with their sharp reduction up to zero point in a thin layer near the wall. The maximal velocity increase above the mean order value is about 10-20 % [27-28]

$$w_{pmax} \approx (1.1\ldots1.2)\,w_{pa}.\qquad(9)$$

It will be shown below, that in the experiment requirements, as a rule, $Re > Re_c$, therefore in the work we shall be restricted by the estimations, performed for the ether turbulent stream.

Let's consider the method operating principle. In the Fig. 1 the part of a cylindrical round metallic tube with the length l_p, which is in the ether stream (ether drift), is shown

The ether stream is shown in the figure as slanting thin lines with arrows, that indicate the direction of its movement. The tube longitudinal axis is located horizontally and along with the ether drift velocity vector is in a vertical plain, which represents the figure plain. The tube walls have major ether-dynamic resistance and the ether stream acting from the tube surface side area, the ether inside a tube does not move. The ether velocity stream stipulated by the horizontal velocity component of the ether drift W_h, creates the ether stream in a tube, which goes with the mean velocity w_{pa}. It can be spoken, that the metallic tube is the routing system for the ether stream. Let's turn a tube in a horizontal plain in such a way, that its longitudinal axis will take up a position perpendicular to

the plain of the Fig. 1 or, that is similar — perpendicular to the velocity vector of the ether drift. In this position both opened ends of a tube will be in identical conditions regarding to the ether stream, the pressure differential Δp does not occur and according to (5) the ether stream velocity in a tube is equal to a zero point. At the moment t_0 we shall turn a tube into the initial position. The horizontal component of the ether drift velocity W_h will create a pressure drop Δp on the tube ends, under operation of which the ether stream will be developed in a tube. In the work [28] the problem about setting into motion of viscous incompressible fluid being in a round cylindrical tube under operating of the suddenly appended constant pressure drop Δp is solved. Let's reduce the formula of the velocity distribution of fluid stream in a tube

$$w_p\left(r,t\right) = w_{pmax}\left[1 - \frac{r^2}{a_p^2} - \right.$$
$$\left. - 8\sum_{k=1}^{\infty}\frac{J_0\left(\psi_k r a_p^{-1}\right)}{\psi_k^3 J_1\left(\psi_k\right)}exp\left(-\frac{\nu\psi_k^2 t}{a_p^2}\right)\right],\qquad(10)$$

where t is the time; ψ_k is the equation roots $J_0\left(\psi_k\right) = 0$; J_0, J_1 are Bessel's functions of the zero and first orders. The first two summands in square brackets express steady (at $t \to \infty$) laminar stream of fluid and correspond the mentioned above "Puazeyl's parabola" (8). So at a turbulent fluid stream, according to (9), the velocity distribution on a tube section is almost uniform, we shall consider, that the fluid stream velocity is equal w_{pa} on the whole tube section (the value γ_p of the round tube at a turbulent fluid stream should be used at the value calculation w_{pa}) except the thin near-wall layer. In this case the expression (10) at $r = 0$ will be like

$$w_p\left(t\right) \approx w_{pa}\left[1 - 8\sum_{k=1}^{\infty}\psi_k^{-3}J_1^{-1}\left(\psi_k\right)\cdot\right.$$
$$\left.\cdot\, exp\left(-\nu\psi_k^2 a_p^{-2}t\right)\right].\qquad(11)$$

The expression (11) describes the process of a fluid stream defining in a round tube. It follows from (11), that at $t \to \infty$ the value is $w_p\left(t\right) \to w_{pa}$. Both parts of the expression (11) should be divided into the value of constant fluid stream velocity in a round tube w_{pa}. In this case the time variation of fluid stream dimensionless velocity $w_p\left(t\right)/w_{pa}$ will be like, that is shown in a Fig. 2.

In the figure the values of dimensionless velocity $w_p\left(t\right)/w_{pa}$ are given on an ordinates axis, the values of time are given on the abscissa axis. As it is shown above, the requirement (2) is performed and the ether stream can be described by the laws of thick liquid motions, then we shall speak about the ether stream further, instead of fluid. In the Fig. 2 we'll allocate the
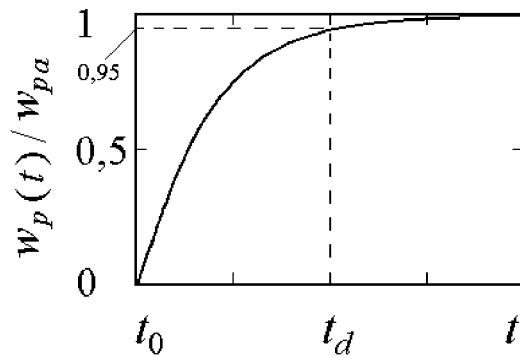
Figure 2: Variation in time of fluid movement velocity in a tube

Figure 3: The schema of an optical interferometer

interval of time $t_0 \ldots t_d$, during which the ether stream velocity in a tube changes from 0 up to 0.95 w_{pa}. We shall call the ether stream regime on this time interval as the dynamic one. We shall call the ether stream regime at $t > t_d$ as the steady stream regime.

Let's skip a light beam along the tube axis. It can be written down, that the phase of a light wave on a cut with the length l_p will vary on value j, which is equal.

$$\varphi = 2\pi f l_p V^{-1}, \tag{12}$$

where f is the electromagnetic wave frequency; V is the light velocity in a tube. According to the original hypothesis the ether is a medium, responsible for electromagnetic waves propagation. This implies, that if in a tube with the length l_p there is the ether stream, the velocity of which changes in time, so the phase of a light wave measured on the tube output, should change in time according to variation in time of the ether stream velocity $w_p(t)$. Then the expression (12) will be like

$$\varphi(t) = 2\pi f l_p \left[c \pm w_p(t) \right]^{-1}, \tag{13}$$

where c is the light velocity in a fixed ether, in vacuum. In the expression (13) the sign "+" is used, when the direction of the light propagation coincides with the ether stream direction in a tube, and the sign "-" is used, when these directions are opposite.

In the work the optical interferometer is applied for measuring value $\varphi(t)$. Rozhdestvensky's interferometer schema is taken [29] as the basis, which is supplemented in such a way, that the light beam drove along the empty metallic tube axis in one of the shoulders. The interferometer schema and its basic clusters are shown in the Fig. 3.

1 — illuminator; 2 — a metallic tube part; 3 — eyefragment with a scale; P_1, P_2 — flat parallel semitransparent laminas; M_1, M_2 — mirrors are shown on the schema. The beam course is shown with thick lines and arrows. The light beam in a tube pass along the axis and is indicated with a broken line in the figure. The tube length is $l_p \approx P_1 M_1$. The clusters P_1, M_1
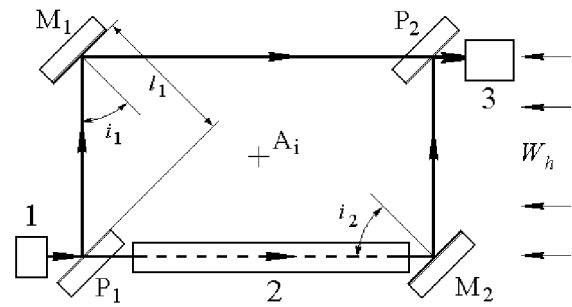
and P_2, M_2 are mounted two by two parallelly, M_1, M_2 are mounted opposite each other on a small angle. The angles i_1, i_2 are the angles between normals to the mirror plains M_1, M_2 and the beams dropping on them. The intervals are $P_1 M_1 = M_2 P_2 = l_1$, $M_1 P_2 = P_1 M_2 \approx l_p$. In a classical case if the ether drift influence isn't considered, the Rozhdestvensky's interferometer operating is reduced to the following. The light beam with the wave length λ is divided P_1 into two beams, which after reflection from M_1 and M_2 and passing P_2 are parallel with a phase difference [29]

$$\delta = 4\pi l_1 \lambda^{-1} \left(\cos i_1 - \cos i_2 \right). \tag{14}$$

The angles i_1, i_2 are established at the interferometer adjustment so that the interference pattern should be observed. (The adjustment clusters are not shown on the schema symbolically). In a tuned interferometer the value is $\delta = const$. In the right part of the Fig. 3 the family of arrows means the stream direction of the ether drift horizontal component velocity. This stream velocity is equal to W_h. If to arrange the interferometer clusters on a horizontal rotated background, such instrument can be turned in the ether stream. The rotation axis is perpendicular to the figure plains and is indicated as A_i.

In the interferometer (Fig. 3) the band position of an interference pattern regarding to the eyefragment scale 3 is defined by the phase difference of the light beams, which are distributed on the paths $P_1 M_2 P_2$ and $P_1 M_1 P_2$. In the Fig. 3 the ether stream is directed towards the light propagation direction along the beams $P_1 M_2$, $M_1 P_2$. In this case, according to (13), we shall write down expression for the phase difference $\Delta\varphi(t)$ between the beams $P_1 M_2 P_2$ and $P_1 M_1 P_2$.

$$\Delta\varphi(t) = 2\pi f \left\{ \left[\frac{P_1 M_2}{c - w_p(t)} + \frac{M_2 P_2}{c} \right] - \left(\frac{P_1 M_1}{c} + \frac{M_1 P_2}{c - W_h} \right) \right\} + \delta, \tag{15}$$

where δ is constant, the value of which is defined by the expression (14). Let's simplify the expression (15).

For this purpose we shall introduce the identifications accepted earlier. Allowing, that the beam phase difference $M_2 P_2$ and $P_1 M_1$ does not depend on the interferometer orientation regarding to the ether stream direction and is equal to zero point, the expression for the value $\Delta\varphi(t)$ will be like

$$\Delta\varphi(t) = 2\pi f l_p \left[\frac{1}{c - w_p(t)} - \frac{1}{c - W_h} \right] + \delta. \qquad (16)$$

The first member of the expression (16) describes the beam phase variation $P_1 M_2$ depending on the ether stream velocity in a tube $w_p(t)$. The second member is the beam phase variation $M_1 P_2$ depending on the ether exterior stream velocity W_h. Let's reduce the expression in square brackets to a communal denominator and, allowing, that $c^2 \gg W_h w_p(t) - c w_p(t) - c W_h$, $fc^{-1} = \lambda^{-1}$ we shall receive

$$\Delta\varphi(t) \approx \frac{2\pi l_p}{\lambda} \left[\frac{w_p(t) - W_h}{c} \right] + \delta. \qquad (17)$$

It follows from the expression (17), that the difference in the phase $\Delta\varphi(t)$ between beams $P_1 M_2 P_2$ and $P_1 M_1 P_2$ is proportional to a differential of the ether stream velocity in a tube $w_p(t)$ and the ether exterior stream W_h.

Let's consider the interferometer operating in its steady regime, at $t \to \infty$. According to the expression (11) and Fig. 2 $w_p(t)_{t\to\infty} \to w_{pa}$ it can be suspected, that owing to the small value of the ether dynamic viscosity (celestial bodies move in the ether) the ether steady stream velocity in a tube regarding to the small length will not differ essentially from the ether exterior stream velocity and it is possible to write down, that $w_p(t)_{t\to\infty} = w_{pa} \approx W_h$. (The correctness of this supposition in the work is determined experimentally and shown below.) In this case in the expression (17) the fraction numerator in square brackets is equal to zero point, and this expression will be

$$\Delta\varphi(t)_{t\to\infty} \approx \delta. \qquad (18)$$

Hence, in the steady regime the interferometer operating with a metallic tube does not differ from the Rozhdestvensky's interferometer operating. In both interferometers the bands position of an interference pattern will be defined by the original phase difference δ. The interferometer, with a metallic tube, in the steady operating regime is not sensitive to the ether drift velocity and can not detect the availability or absence of the ether drift.

Let's consider a dynamic operating regime of the interferometer. Let's unroll the interferometer (see Fig. 3) in the horizontal plain at $180°$. As the direction of the light propagation has varied in relation to the ether drift stream to the opposite one, the expression (17) will be like

$$\Delta\varphi(t) \approx \frac{2\pi l_p}{\lambda} \left[\frac{W_h - w_p(t)}{c} \right] + \delta. \qquad (19)$$

According to the expression (11) and the Fig. 2, the inequality $w_p(t) < W_h$ takes place at the time interval $t_0 \ldots t_d$. Hence, in a dynamic regime the interferometer with a metallic tube is sensitive to the velocity differential of the ether exterior stream velocities W_h and the ether stream inside a tube $w_p(t)$. We shall discover the bands offset value of the interference pattern regarding to their position in the interferometer steady work regime as follows. Let's take a differential of the expressions (19), (18) and divide both parts of the found expression into 2π, we shall receive

$$\frac{\Delta\varphi(t) - \Delta\varphi(t)_{t\to\infty}}{2\pi} = \frac{l_p}{\lambda} \left[\frac{W_h - w_p(t)}{c} \right]. \qquad (20)$$

The expression left-hand part (20) is equal to the required interference pattern offset, which is expressed by the number of electromagnetic wave periods. With reference to the visually observed interference pattern the expression (20) describes the value variation in time of visible bands offset of this pattern regarding to their original position — $D(t)$. The visible bandwidth value of an interference pattern can be the offset measurement unit. Taking into consideration, that the ether stream in a tube can have the direction opposite to the selected on the Fig. 3, generally it is possible to receive

$$D(t) = \pm \frac{l_p}{\lambda} \left[\frac{W_h - w_p(t)}{c} \right]. \qquad (21)$$

In the expression (21) the sign ”+” is used, when the light propagation direction coincides with the ether stream direction in the interferometer dynamic regime in a tube, and the sign ”-” is used, when these directions are opposite. According to the expression (11) and the Fig. 2 at an instant $t_0 = 0$ the ether stream velocity in a tube is $w_p(t_0) = 0$. Then from (21) we shall receive, that at the instant t_0 the bands offset of an interference pattern accepts the maximal value equal to

$$D(t_0) = \pm \frac{l_p}{\lambda} \cdot \frac{W_h}{c}, \qquad (22)$$

and in the steady regime, when the ether velocity in a tube is equal to $w_p(t)_{t\to\infty} \approx W_h$, the bands offset regarding to their original position is equal 0. The dependence view $D(t)$ can be obtained with the dependence $w_p(t)/w_{pa}$, which is shown in the Fig. 2. Really, let's divide (21) into (22), we shall receive

$$\frac{D(t)}{D(t_0)} = 1 - \frac{w_p(t)}{W_h}. \qquad (23)$$

Allowing the supposition made above, that $w_p(t)_{t\to\infty} = w_{pa} \approx W_h$ the expression (23) can be written down as $D(t)/D(t_0) \approx 1 - w_p(t)/w_{pa}$. The dependence view obtained in such a way, is shown in the Fig. 4

In the expression (22) the measured value D is proportional to the first extent of the ether drift velocity ratio to the light velocity, that characterizes the reviewed
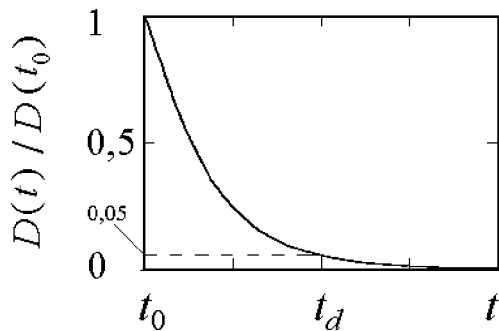
Figure 4: Variation in time of interference pattern bands offset in a dynamic interferometer operating regime

method as the first order method. It follows from the expression (22) and the Fig. 4, that if at the moment of time t_0 to measure the bands offset value D regarding to their original position on the interferometer eyefragment scale, it is possible to determine the ether drift velocity horizontal component W_h which is equal to

$$W_h = \pm D\left(t_0\right) c\lambda l_p^{-1}, \tag{24}$$

The direction of the interference pattern bands offset, regarding to their original position, will be defined by the ether exterior stream direction.

The data of the interferometer tube sizes are necessary for the proposed measuring method realization. The expression for the tube interior radius calculation a_p can be obtained as follows. Let's divide both parts of the expression (11) on w_{pa} and, allowing, that at the moment of time t_d (see the Fig. 2) the ratio $w_p\left(t\right)/w_{pa} = 0.95$, we shall write down as

$$1 - 8\sum_{k=1}^{\infty}\psi_k^{-3}J_1^{-1}\left(\psi_k\right)exp\left(-\nu\psi_k^2 a_p^{-2}t_d\right) =$$

$$= 0.95. \tag{25}$$

If to be confined by the estimation accuracy no worse than 7 %, so the series in the expression (25) can be exchanged by its first member. Let's substitute in the (25) the numerical values ψ_k and $J_1\left(\psi_k\right)$ (for the information we shall give these values: $\psi_1 = 2.4048$; $J_1\left(\psi_1\right) = 0.5191$), we shall receive

$$a_p \approx 1.37\left(t_d\nu\right)^{1/2}. \tag{26}$$

The expression (26) allows to calculate such the interferometer design parameter as the tube radius a_p. At calculation, the value t_d is selected coming from the time, which is required for implementation of visual (or tool) readout of bands offset value D. The data of the ether kinematic viscosity value v will be reviewed

below. The tube length l_p can be found with the expression (24), of which we shall receive

$$l_p \approx D_{min}\left(t_0\right)\lambda c W_{hmin}^{-1}, \tag{27}$$

where $D_{min}\left(t_0\right)$ is bands offset minimum value of an interference pattern, which can be digitized with the selected eyefragment and scale; W_{hmin} is the minimum value of the ether drift horizontal component velocity, which should be measured by the interferometer (the interferometer sensitiveness).

The ether kinematic viscosity. The data of the ether kinematic viscosity value v are necessary for the measuring method realization. Let's estimate the value v, relying on the following. In the work [5] the photon formation mechanism is represented, as the oscillating result of excited atom electronic shell in the ether and the Karman's vortex track as hydromechanical photon model is proposed. In other words the photon formation is stipulated by the ether stream turbulent regime of the excited atom streamlining by the ether, oscillating in the ether. The turbulent pulsation propagation in the ether is perceived by the observer as the light emission. In the work [28] it is shown, that the existence of pulsation movement is possible in fluid volume, if the Reynold's number is not lower than some extreme value equal to

$$Re_{cr} = wd\nu^{-1}, \tag{28}$$

where w is fluid movement velocity; d is the characteristic size of a streamlined body. In the work [28] it is obtained, that $Re_{cr} \approx 425$. With reference to our problem the values w, d, v are accordingly: the ether movement velocity, atom diameter, the ether kinematic viscosity. From the expression (28) we shall find

$$\nu \approx wdRe_{cr}^{-1}. \tag{29}$$

We shall call the obtained ether kinematic viscosity value as the calculated ether kinematic viscosity value v_c. Let's calculate the value v_c. As the ether stream velocity w we shall accept the offset velocity of electronic atom shells in the immobile ether at a photon emission. Let's consider, that this velocity does not exceed the light velocity $w \leq c$. The diameter of atoms, as it is known, has the value order $d \approx 10^{-10}$ m. In this case with the (29) we shall receive

$$\nu_c \leq 7.06 \cdot 10^{-5} \text{ m}^2\text{sec}^{-1}. \tag{30}$$

The performed estimation has shown, that the ether kinematic viscosity calculated value corresponds to the work imaginations [6] about the ether as gas-like medium with real gas properties. So, the kinematic viscosity values of twelve gases, spread in nature, are within $7 \cdot 10^{-6}$ m^{2}sec^{-1} (carbon dioxide) up to $1.06 \cdot 10^{-4}$ m^{2}sec^{-1} (helium).
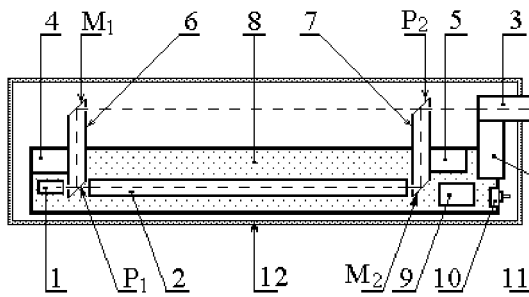
Figure 5: The interferometer structure

Optical interferometer. The calculated ether kinematic viscosity value allows to calculate the interferometer parameters. With the expression (26) we shall determine the tube radius. If the value t_d is supposed to be equal 1 second, we shall receive, that at the interferometer creation it is necessary to apply the tube with the interior radius $a_p \approx 0.05$ m. We shall determine the tube length l_p with the expression (27). If to suppose the values $D_{min} = 0.05$, $W_{h\,min} = 20$ m/sec and apply the light source with the wave length $\lambda = 6.5 \cdot 10^{-7}$ m, so the required tube length is equal to $l_p \approx 0.49$ m.

The optical interferometer was manufactured for conducting measurements. Schematic figure of the device (the top view) is shown in the Fig. 5.

In the Fig. 5 the identifications of the basic clusters are kept, which were introduced at viewing the interferometer schema (Fig. 3). 4,5 — the interferometer adjustment clusters; 6,7 — racks for fixing flat-parallel semi-transmitting laminas and mirrors; 8 — interferometer frame; 9 — power supply accumulators of the illuminator; 10 — the illuminator switch; 11 — the eyefragment fixing cluster; 12 — heat-insulating housing are shown additionally. The frame 8 is manufactured of a steel profile with П — like section. The wall thickness is 0.007 m. The profile height is 0.02 m. The frame length is 0.7 m, the width is 0.1 m. The interferometer clusters are fixed on a flat frame surface. The racks 6, 7 are manufactured of rectangular copper tubes with interior section 0.01 m × 0.023 m. The light beams pass inside these tubes. The interval between beams is $P_1 M_2$ and $M_1 P_2$ it is equal 0.12 m. On racks, in the points P_1, P_2 the flat parallel semi-transmitting laminas, in the points M_1, M_2 — mirrors are installed. (In the manufactured interferometer the flat parallel glasses with the thickness 0.007 m were used as semi-transparent laminas). The laminas, mirrors and clusters of their fixing in the Fig. 5 are not shown symbolically. Each of the clusters 4,5 allows to change the racks position in two orthogonal related plains. The tube 2 is steel with the interior radius $a_p = 0.0105$ m. The

tube length is $l_p = 0.48$ m. The clusters of the tube fixing on 5 are not shown symbolically. The semiconductor laser with the wave length $\lambda \approx 6.5 \cdot 10^{-7}$ m was applied as the illuminator. The optical paths in the interferometer are located in a horizontal plain. The interferometer was located on a rotated material table, which was manufactured of an organic glass with the thickness 0.02 m. The heat-insulating gasket was put between the frame and material table . The interferometer was closed by a common housing of six layers of a soft heat-insulating material. The thickness of such coating was about 0.025 m. In the Fig. 5 the housing perimeter is shown. The housing background was the box of rectangular section with the interior sizes: width $b_c = 0.22$ m, height $h_c = 0.11$ m, length $l_c = 0.8$ m. The box was manufactured of a cardboard with the thickness 0.007 m. In the box the face wall on the eyefragment part was absent. This opening was closed with a common soft housing. The interferometer rotating was ensured with the end thrust bearing of the diameter 0.075 m. The bearing box is located between the material table and support. The support is provided with the units for the interferometer installation in a horizontal position.

The interferometer test. In the manufactured interferometer the minimum bands offset of an interference pattern, which could be visually digitized, meant $D_{min} = 0.05$.

The device stiffness was tested by two methods. According to the first method the instrument frame was mounted on a horizontal surface. The interferometer for one edge of a frame was hoisted in such a way, that the frame lean angles to the surface plain reached $\approx 20°$. In this position the interference patterns offset frame, stipulated by elastic deformations of the instrument, did not exceed 0.3 bands ($D = 0.3$). According to the second method the instrument stiffness was tested in a working position. The frame lean angles up to $10°$ were created by the material table tilt. In this case the bands noticeable drift was not observed. The stability of an interference pattern to impulsive loads was tested. The light shocks on the interferometer frame, material table and support caused short-lived interference pattern wince at the moments of such strikes. Thus the interference pattern was not destroyed. The bands saved an original position after termination of impulsive loads.

The second stage of tests was performed on the terrain selected for experimental investigations. In windy weather the interference pattern was stable. The observer moving in an immediate proximity from the interferometer installation site, the movement of the pedestrians and cars in 20 meters from the instrument installation site did not cause the noticeable offset or bands shivering. The short-lived bands shivering at cars movement was marked on one of two selected points, which was in seven meters from a ground road. Thus the interference pattern was observed, and the bands

did not change the position. (The transport movement in this terrain is insignificant — on the average 3-4 automobiles per a day.)

The interferometer heat tests were held in summer. The device was mounted on the open site. The various device orientation on an azimuth was set in cloudless weather conditions. In a fixed position the instrument was heated by solar radiation. In these conditions within 30 minutes the bands offset did not exceed the value $D = 0.35$ ($\approx 1/100$ bands for a minute). In cloudy weather and at night the interference pattern saved an invariable position within 2-3 hours.

The measuring method sensitiveness to the ether drift required effects was tested at the test final stage. The method of interferometer application was the following. The instrument was mounted in a horizontal position in such a way, that its direct axis coincided with a meridian line, and the illuminator was turned to the north. In such initial position, in the interferometer steady work, the observer registered the bands original position of an interference pattern regarding to the eyefragment scale. The value $D = 0$ was given to the bands original position. Then the observer changed the position — took a seat at the illuminator. The interferometer turned in $180°$. The rotational displacement was performed within three seconds. At rotational displacement, as it was reviewed above, the ether stream in a tube was interrupted. The interferometer transferred into a dynamic operating regime, which is described by the expression (11). In this interferometer position the maximal value of bands offset, the bands release time to their original position was registered. The interferometer transferred into a steady regime, and turned into the initial position. At this stage of tests it was established, that after the dynamic regime termination the bands noticeable offset of an interference pattern regarding to their original position was not observed, i.e. bands offset value $D(t)_{t \to \infty} \approx 0$. According to the expression (21) it means, that the ether stream velocity along the tube axis at $t \to \infty$ differed a bit from the ether exterior stream velocity, that the value D was behind the interferometer threshold. It can be explained by small resistance of the interferometer tube to the ether stream movement inside this tube. Let's consider in this case, that

$$w_p(t)_{t \to \infty} = w_{pa} \approx W_h. \qquad (31)$$

This experimental result was used above at the proportion deduction (18).

At procedure implementation, described above, it was marked, that at the whole time course of value D variations corresponded to variations, which are shown in the Fig. 4 that did not contradict the original imaginations about the interferometer work. The measured duration of a dynamic regime meant $t_d \approx 10 \ldots 13 sec$. The values ambiguity t_d is stipulated, first of all, by the
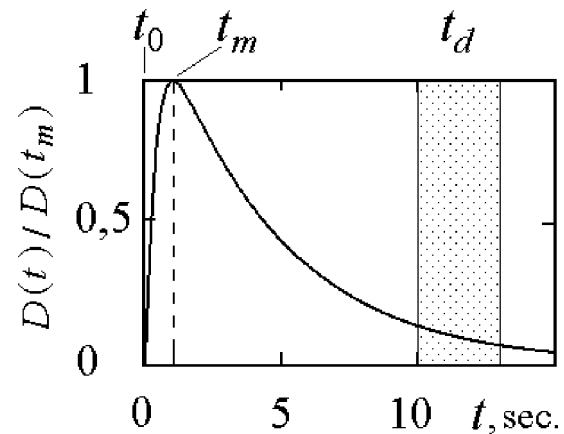

Figure 6: Observed variation in time of the interference pattern bands offset in the interferometer dynamic operating regime

difficulties, connected with small values visual readout of the value D, slowly changing, at the dynamic regime end, i.e. at $t \to t_d$. In the Fig. 6 the dependence view $D(t)$, created on the data visual observations, is shown.

However, as it can be seen in the Fig. 6, on the original site by the extent about 1 second the dependence time course $D(t)$ differed from an expected time course qualitatively. After the device rotation in $180°$, at the moment of time t_0, the bands still occupied the initial position, i.e. $D(t_0) = 0$ instead of anticipated, according to (22) and the Fig. 4, the value $D(t_0) = max$. Since the moment t_0, the value D within the time $t_m \approx 1sec$ reached the maximal value. There were suppositions of certain mechanical stresses influencing at the interferometer braking after its rotation in $180°$ or other reasons, connected, for example, with air movement inside a heat-insulating housing. In this connection different methods of the interferometer starting into movement and its braking were tested. The tests have shown, that the observed feature of the interferometer work could not be explained by the suppositions made. The systematic round-the-clock tests have shown the following. The daily variations of the value D corresponded the measured ones in the experiment [1-3] to the ether drift velocity variations within a day. (In the experiment [1-3] round-the-clock measurements were carried out continuously during 13 months, since August 1998 till August 1999. The part of this experiment results is published in the works [1-3]. The measurement results within radio waves band have shown, that there is a rather small value of the ether drift horizontal component velocity during the part of a day. The same effects were marked at the optical interferometer test in the work. The experience has shown, that at a separate day, on such periods of time at the interferometer rotation on $180°$ the no-

ticeable bands offset of an interference pattern was not observed. Hence, the detected features in dependence $D(t)$ (Fig. 6) could not be caused by the interferometer mechanical strains or air movements inside the interferometer heat-insulating housing, and are stipulated by the exterior reasons. Such time periods, during which $D(t_m) \approx 0$ were used for improvement ways of the interferometer starting in rotation and its stopping. These ways were used then as standard procedures at systematic measurement conducting.

Analysis of the interferometer test results. The detected regularity in the observed bands offset has required its physical interpretation. The possible influencing analysis of the interferometer structural elements on the ether streams has shown, that the observed dependence features $D(t)$ can be qualitatively and quantitatively described within the following supposition. Let allow, that an exterior heat-insulating dielectric housing of the interferometer (the point 12 in the Fig. 5) forms the additional directing system for the ether stream drift, besides a metallic tube. In this case the exterior in relation to a metallic tube of the ether stream is the ether movement in a dielectric housing. If to consider the interferometer housing as the routing system, it is necessary to consider, that, since the moment t_0 in it, as well as in a metallic tube, the dynamic process of the ether stream defining will be developed. It gives the basis to write down the expression (21) as follows

$$D(t) = \pm \frac{l_p}{\lambda} \left[\frac{W_c(t) - w_p(t)}{c} \right], \qquad (32)$$

where $W_c(t)$ is the variation of the ether stream velocity in time in the interferometer housing; $w_p(t)$ is the variation of the ether stream velocity in time in a metallic tube.

The housing basis was a cardboard box of rectangular section. Let's consider a problem about setting the ether into motion, resting in a rectangular tube. For this purpose let's use the comparative method, spread in hydrodynamics, of fluid stream in a tube of a compound profile with fluid stream in the tube of round section, "equivalent" on resistance, at which so-called "hydraulic" radius a_h equal to an area ratio of a tube normal section G_p to the section perimeter N_p is accepted [27] for this radius

$$a_h = G_p N_p^{-1}. \qquad (33)$$

Such a way enables to use the mathematical apparatus developed at stream analysis in round tubes. As before we shall be limited to estimations, performed for the ether turbulent stream. In this case the dependence $W_c(t)$ can be calculated with the expression similar to the expression (11) in which as the round tube radius

a_p we shall use the "hydraulic" radius of a rectangular tube a_h

$$W_c(t) \approx w_{pac} \left[1 - 8 \sum_{k=1}^{\infty} \psi_k^{-3} J_1^{-1}(\psi_k) \cdot \right.$$
$$\left. \cdot exp\left(-\nu \psi_k^2 a_h^{-2} t\right) \right], \qquad (34)$$

where w_{pac} is a mean velocity of the ether steady turbulent stream in the interferometer dielectric housing. As before, at considering the expression (17), and taking into account the interferometer test results (31), it is possible to consider, that the value w_{pac} does not differ essentially from the ether exterior stream velocity W_h and it is possible to write down

$$W_c(t)_{t \to \infty} = w_{pac} \approx W_h. \qquad (35)$$

Let's calculate the value a_h. Above, the housing interior overall dimensions were given at the interferometer structure description: width $b_c = 0.22$ m, height $h_c = 0.11$ m. Then, having determined the values G_p and N_p, with the (33) we shall receive $a_h = 0.0367$ m.

From the expression (26) it is possible to see, that the duration of the interferometer dynamic regime t_d will be defined by the tube of larger radius. As $a_h > a_p$, the value t_d will be defined by the value of "hydraulic" radius of the interferometer housing a_h

$$t_d \approx 0.53 a_h^2 \nu^{-1}. \qquad (36)$$

From the expression (36) it follows, that, having the measured values t_d, it is possible to determine the ether kinematic viscosity value

$$\nu \approx 0.53 a_h^2 t_d^{-1}. \qquad (37)$$

The kinematic viscosity value, determined in such a way, we shall call as the ether kinematic viscosity measured value v_c. Let's substitute into (37) the values $a_h = 0.0367$ m and the measured value $t_d = (10 \dots 13)$ sec, we shall receive

$$\nu_e \approx (5.5 \dots 7.1) \cdot 10^{-5} \text{ m}^2\text{sec}^{-1}. \qquad (38)$$

The kinematic viscosity mean value v_{ea}, calculated as the function mean value $v = f(t_d)$ within $(10 \dots 13)$ sec is equal to

$$\nu_{ea} = 6.24 \cdot 10^{-5} \text{ m}^2\text{sec}^{-1}. \qquad (39)$$

Comparing (30), (38) and (39) we shall mark, that on the value order the ether kinematic viscosity values, calculated and measured, coincide $v_c \approx v_e \approx v_{ea}$.

The opportunity of the problem solution about the ether viscosity measuring is of particular interest, as the experimental data about the ether viscosity and the ether viscosity measuring methods miss in literature till nowadays.
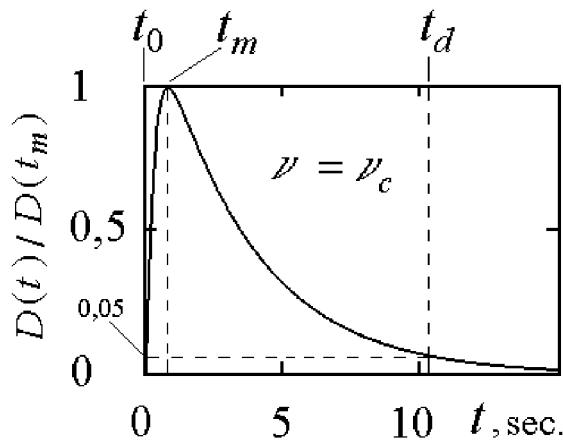
Figure 7: Variation in time of the interference pattern bands offset (calculation)

Let's write down the expression for the value $D(t)$. For this purpose we shall substitute the expressions (11) and (34) in (32) for the values $w_p(t)$ and $W_c(t)$ accordingly and, allowing the proportions (31), (35), we shall receive

$$D(t) \approx \pm \frac{8l_p W_h}{\lambda c} \sum_{k=1}^{\infty} \psi_k^{-3} J_1^{-1}(\psi_k) \cdot$$

$$\cdot \left[exp\left(-\nu \psi_k^2 a_p^{-2} t\right) - exp\left(-\nu \psi_k^2 a_h^{-2} t\right) \right]. \qquad (40)$$

In the Fig. 7 in a normalized view the dependence calculation result $D(t)$, performed with the expression (40) is given. At calculations the terms number of a series $k = 4$, the calculated value of the ether kinematic viscosity is $v_c = 7 \cdot 10^{-5} m^2 sec^{-1}$ and the following values of the interferometer design parameters are used: $a_p = 0.0105$ m; $a_h = 0.0367$ m; $l_p = 0.48$ m; $\lambda = 6.5 \cdot 10^{-7}$ m.

From the Fig. 7 it follows, that on time expiration $t_m \approx 0.82$ sec, which is digitized from the moment t_0 of the beginning time of the interferometer dynamic operating regime, the bands offset maximal value of the interference pattern (value D) should be observed. The anticipated duration of the interferometer dynamic operating regime matters $t_d \approx 10.3$ sec. Let's use the expression (40) for specifying the observed value experimentally $t_m \approx 1$ sec. For this purpose we shall substitute in (40) the measured value of the ether kinematic viscosity, $v_{ea} = 6.24 \cdot 10^{-5}$ m^{2}sec^{-1}, we shall receive $t_m \approx 0.93$ sec. Hence, the calculation results do not contradict the experience results, which are shown in the Fig. 6.

The interferometer test results analysis, the ether kinematic viscosity values, calculated and measured, give the basis to consider, that the ether stream properties are close to the stream properties of known gases at their interaction with solids — to pass aside obstacles

and go in directing systems. It can be suspected, that solids (dielectrics, metals etc.) at interaction with the ether stream render major ether-dynamic resistance. It clarifies the interferometer test results, that the tube made of dielectric can execute the same directing system role for the ether, as the tube made of metal. The ether stream property, i.e. to pass aside obstacles, could cause unsuccessful attempts to detect the ether drift with the devices placed in metallic chambers [17-20, 23-26].

For value definition of the ether drift horizontal component velocity W_h it is possible to use the bands offset measured value of an interference pattern at the moment of time t_m, when $D(t_m) = max$. From the expression (40) we shall receive

$$W_h \approx D(t_m) \lambda c \left\{ 8l_p \sum_{k=1}^{\infty} \psi_k^{-3} J_1^{-1}(\psi_k) \cdot \right.$$

$$\left. \cdot \left[exp\left(-\nu \psi_k^2 a_p^{-2} t_m\right) - exp\left(-\nu \psi_k^2 a_h^{-2} t_m\right) \right] \right\}^{-1}. \quad (41)$$

Let's substitute in (41) the measured values of the ether kinematic viscosity $v_{ea} = 6.24 \cdot 10^{-5}$ m^{2}sec^{-1}, the value $t_m = 1$ sec, the design parameters value of the interferometer and calculation parameter (the terms number of a series): $a_p = 0.0105$ m; $a_h = 0.0367$ m; $l_p = 0.48$ m; $\lambda = 6.5 \cdot 10^{-7}$ m; $k = 4$. In this case the measured value of the ether drift horizontal component velocity, will be defined as follows

$$W_h \approx 525 D(t_m). \qquad (42)$$

Let's calculate the minimal value of the ether drift velocity W_{hmin}, which can be measured with the manufactured interferometer, i.e. we shall determine the instrument sensitiveness. In the part "the interferometer test" is marked, that the minimum value D_{min}, which can be digitized with the selected eyefragment and scale $D_{min} = 0.05$. Then with the expression (42) we shall receive $W_{hmin} = 26.25$ m/sec.

Let's determine the ether stream regime in the interferometer tubes at $W_h = W_{hmin}$. For this purpose with the expression (4) we shall calculate the minimal value of the Reynolds number Re_{min} for the tube with radius $a_p = 0.0105$ m, in which the ether with the viscosity $v_{ea} = 6.24 \cdot 10^{-5}$ m^{2}sec^{-1} moves. Let's receive $Re_{min} \approx 8834$. According to the requirement (3) it can be written down, that $Re_{min} > Re_c$. Hence, at the ether drift velocities $W_h \geq 26.25$ m/sec the ether stream turbulent regime is possible only in the interferometer tubes.

The optical interferometer tests and tests results analysis give the basis to consider, that the hydrodynamic description of the interferometer operating principle, reviewed above, is adequate to the imaginations about viscous ether stream in tubes, and the manufactured interferometer is suitable for the ether drift velocity and the ether kinematic viscosity measuring.

The measurement methods. The interferometer was disposed in the country settlement at the height ($\approx$ 190 m above sea level), in 13 km from Kharkov northern suburb. The proximate height ($\approx$ 200 m above sea level) is located westward apart 1.7 km. Two points were arranged for measurements. The distance between them was about 15 m. On the point No 1 the interferometer was at the height 1.6 m above the ground surface. On the point No 2 it was at the height 4.75 m. Two points available, which are located at different heights and are practically at the same point of terrain, it is required for observation of the "height effect." The measurements on the points No 1 and No 2 were performed in the open air. On the point No 1 the interferometer was in surrounding trees shadow and was not exposed to direct solar radiation affecting within a light day. On the point No 2 the interferometer was mounted in an umbrella shadow. In winter time the interferometer was transferred to Kharkov. The point No 3 ($\approx$ 30 m above the ground surface or $\approx$ 130 m above sea level) was arranged in the upper level facility of a bricky house. On the point No 1 the measurements were carried out in August 2001, on the point No 2 in August, September, October and November 2001, on the point No 3 in December 2001 and in January 2002.

The measurements were carried out cyclically. One measuring cycle lasted 25-26 hours. 2-4 cycles were performed within one month. Each cycle contained the following parameters. The interferometer was mounted on a selected point, so that its rotating plain was horizontal. After installation the interferometer was kept in new heating environment within one hour (the instrument was stored in the facility). The measurements were carried out at each whole hour of stellar time. One readout of the measured value was performed under the following schema. The interferometer longitudinal axis was mounted along a meridian, so that its illuminator was turned to the north. The further procedures did not differ from the interferometer operating procedures, which were applied at the final stage of the interferometer test. After the interferometer dynamic regime termination the observer registered the maximal bands offset value $D(t_m)$, as the measured value. The bands release time to their original position was registered and metered. The interferometer returned to the steady operating regime. The instrument turned to the initial position. As a rule, 5-7 readouts were done during one measuring time ($\approx$ 10 minutes). The readout mean value was accepted for the measured value $D(S)$, where S is the measuring stellar time.

The processing methods of the measurement results. The measurement results processing included the following procedures: values calculations of the ether drift horizontal component velocity W_h; a daily course of the ether drift velocity within separate stellar day and the ether drift velocity daily course averaged during the year epoch $W_h(S)$; a daily course of the

ether drift velocity averaged for the whole time of the measurement series $\overline{W_h(S)}$, mean-square value deflection W_h from its mean value σ_W.

The measurement results were introduced as the measured value tables $D(S)$. The values W_h, calculated with the expression (42) were brought to the same table for each hour of stellar day. Such numbers consequence obtained for separate stellar day, describes a daily course $W_h(S)$.

The mean values of the ether drift velocity and the values σ_W were calculated for each hour of the stellar day with the following known expressions [30]

$$\overline{W_h(S)} = \rho^{-1} \sum_{j=1}^{\rho} W_{hj}(S), \qquad (43)$$

$$\sigma_W(S) = \left\{ \rho^{-1} \sum_{j=1}^{\rho} \left[W_{hj}(S) - \overline{W_h}(S) \right]^2 \right\}^{1/2}, (44)$$

where ρ is the values amount W_h, obtained during the whole measurement series. The confidence intervals of the measured values were calculated with the known methods explained, for example, in the work [30]. The calculations were performed with the estimation reliability equal to 0.95.

The measurement results. The measurement series results, held since August 2001 till January 2002 are presented in the work. 2322 readouts of the measured values have been performed during this series. The distribution of readouts amount per months of the year is shown in the table 1

According to the research problems, we shall consider this work results along with the experiment results [1-3], [7-9], [10]. These four experiments have been performed at various points of a globe with three different measuring methods: an optical interferometer of the first order (Europe, Ukraine, 2001–2002 [this work]); a radio interferometer of the first order, (Europe, Ukraine, 1998–1999 [1-3]); optical interferometers of the second order (Northern America, USA, 1925–1926 [7-9], 1929 [10]). The measuring methods action, which are applied in the above-mentioned experiments, based on wave propagation regularities in moving medium, responsible for these waves propagation, that allows to treat the experiment results in the terms of the ether drift velocity within the original hypothesis.

The development regularities of viscous medium streams (fluids or gases) in directing systems are used in the work measuring method. The measured value is proportional to a velocity differential of the ether viscous streams in two tubes of different section within the original hypothesis. This differential value is proportional to the ether drift velocity (the first order method).

In the experiment measuring method [1-3] the regularities of viscous medium streams near the surface

Table 1: Distribution of readouts amount per months of the year

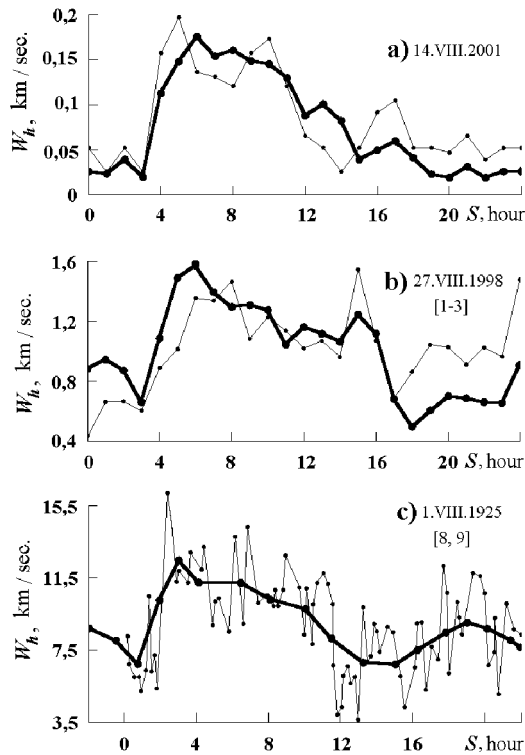| Month of the year	August 2001	September 2001	October 2001	November 2001	December 2001	January 2002
Amount of readouts	792	462	288	312	240	228

Figure 8: Variation of ether drift velocity within a day in August epoch

partition are used. The measured value is proportional to a vertical velocity gradient in the ether drift stream near the Earth's surface within the original hypothesis. This gradient value is proportional to the ether drift velocity (the first order method).

In the experiments [7-9] and [10] Michelson's cruciform interferometers were applied. The measured value is proportional to a velocity differential of wave propagation in orthogonal related directions in the ether drift stream within the original hypothesis. This differential value is proportional to the ether drift velocity (the second order method).

In the Fig. 8 the experiment results referring to August are presented. On fragments of this figure are shown accordingly: in the Fig. 8a — this work results; in the Fig. 8b — the experiment results [1-3] (the figure is published for the first time); in the Fig. 8c — the experiment results [7-9].

The ether drift velocities W_h in km/sec. are pending on ordinate axes. The stellar time S in hours is

pending on abscissa axes. Each of the Fig. 8 fragments illustrate the variation of the ether drift velocity within a stellar day W_h (S). The experiment results are presented only by the authors of work [10] as ascertaining of the velocity maximal value, measured by them, in relation to the movement $W \approx 6$ km/sec, that has not allowed to show this experiment results in the Fig. 8 as the daily dependence W_h (S). In the Fig. 8 the measurement data averaging results were presented with the thick lines, which are obtained in each of the experiments during August epoch (mean results). The separate observations (measurement results during a separate day) are shown with thin lines. The dates of separate observations are specified on fragments. The separate observations on fragments of the Fig. 8a, Fig. 8b are selected from the performings, which had the date, proximate to the date of separate observation of the Fig. 8c fragment and which during the day had no skips during the measuring. The date discrepancy is stipulated also by the fact that the systematic measurements in the work began on August 14, 2001, and in the experiment [1-3] — on August 11, 1998.

The positive measurement results, given in the Fig. 8, illustrate the development of anisotropy effect — the ether drift required effect. In the work and in the experiments [7-9], [10] the anisotropy effect was discovered by the optical interferometer rotation, in the experiment [1-3] the opposing radio waves propagation was applied.

The similar nature of the ether drift velocity variation within a day in August epoch unite all three fragments of the Fig. 8. The first minimums in dependencies W_h (S) are expressed clearly in all three mean results. In the work (Fig. 8a) and in the experiment [1-3] (Fig. 8b) temporary position of minimums is $S \approx 3$ hours. In the experiment [7-9] (Fig. 8c) the temporary position of the first minimum is $S \approx 0.8$ hour. (Such discrepancy in the position of these minimums is about 2.2 hour, an explanation has not found yet.) The ether drift velocity magnification is observed during consequent 2-3 hours. Further the plateau sites with rather small variations of the ether drift velocity in time are noticed on all fragments. The greatest duration of the plateau site was observed in the experiment [1-3] (Fig. 8b), that can be explained by arranging peculiarities of a radio-frequency spectral line on terrain. In this experiment the radio-frequency spectral line is declined from a meridian on 45° to northeast. The variations

of the ether drift apex azimuth (as well as any star azimuth) occur symmetrically to a meridian line within a stellar day. If to take the apex coordinate values into account (according to Miller: $\delta \approx 65°$, $a \approx 17.5^h$ [9]), the ether drift azimuth in this part of a stellar day accepts the values, which lay in the northeast direction, i.e. in the direction close to the direction of a radio-frequency spectral line. In this case the angle between the ether drift azimuth and radio frequency spectral line direction has minimum values. Accordingly at the interval of 12-16 hours the ether drift radial component velocity (directed along a radio-frequency spectral line) keeps rather high value, despite of the apex height magnification (astronomical coordinate). Such arranging peculiarities of the radio interferometer on terrain can explain the relative dependence increase $W_h(S)$ at the interval of 12-16 hours in comparison with the same dependencies shown on two other fragments. In the work (Fig.8a), according to the accepted measurement methods, the optical interferometer was located along a meridian. As the variations of the ether drift azimuth within a stellar day occur symmetrically to the meridian line, in this case the plateau site duration should be less, than in the experiment [1-3] and less than in the experiment [7-9] in which the ether drift azimuth variation was considered by the corresponding rotation of the interferometer.

It can be seen in the Fig. 8a (the mean result of the work), that the sites with rather small values of the ether drift velocity, extended in time, take place within a day. Noticeable bands offset of an interference pattern was not observed per a separate day on such sites. In these cases the ether drift velocity was lower than the interferometer sensitiveness (i.e. $W_h < 26$ m/sec), that was used for the interferometer tests, the purpose of which is given in the above mentioned part "the interferometer test".

Systematic character of experimental investigations of this work and the works [1-3], [7-9] has shown, that dependencies measured in one and the same epoch of the year $W_h(S)$, have the similar character of the ether drift velocity variation within a day. At the same time dependencies view $W_h(S)$, measured in different epochs of the year differ from each other, that can be noticed, for example, by the experiment published results [7-9]. The reasons of such seasonal variations have not been defined yet. It can be suspected, that magnetosphere, at its considerable sizes and peculiar shape, ionosphere, the known variations of their state can be responsible for such dependence variations $W_h(S)$.

It can be seen in the Fig. 8, the ether drift velocities, measured in each of the experiments, differ, that can be stipulated by the arranging height differences of measuring systems above the Earth's surface: 1.6 m; 42 m; 1830 m (Fig. 8a, Fig. 8b, Fig. 8c accordingly). The collection of such data illustrates the height effect development. In the work the ether drift velocity mea-
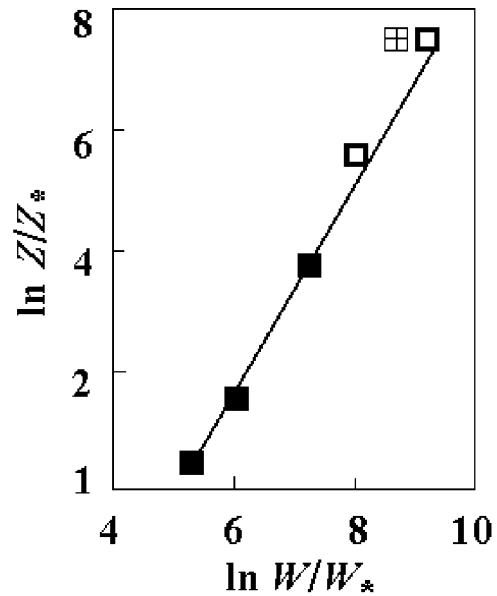
Figure 9: Dependence of the ether drift velocity on the height above the Earth's surface, ■ is this work and experiment [1-3]; □ is the experiment [7-9]; ⊞ is the experiment [10]

suring have been performed at the heights 1.6 m and 4.75 m (position No. 1 and No. 2) for height dependence discovery. In the table 2 the mean values of the ether drift maximal velocity are given, which are measured in the work and in the experiments [1-3], [7-8], [10]. In these four experiments the measurements are performed at five different heights: 1.6m and 4.75 m in the work; 42 m in the experiment [1-3]; 265 m and 1830 m in the experiment [7-9] (Clevelend and the observatory of Mount Wilson accordingly). In the experiment [10] the measurements were carried out also on the observatory of Mount Wilson. However, in contrast with the experiment [7-9], which was carried out in a light wooden house, the experiment [10] is performed in a fundamental building of an optical workshop of the observatory. It can be supposed, that the ether stream braking by the house walls was the reason of the ether drift velocity smaller value, measured in the experiment [10] in comparison with the experiment result [7-9].

The table 2 gives the imagination about the ether drift velocity variation in height band above the Earth's surface from 1.6 m up to 1830 m. In the figure 9 this dependence view is presented in the logarithmic scale. On the abscissa and ordinates axes the logarithmic values of ratios W/W_* and Z/Z_* were pending accordingly, where: W is the ether drift velocity at the height Z; the values W_* and Z_* are considered equal to 1 m/sec and 1 m accordingly.

Table 2: Dependence of the ether drift velocity on the height above the Earth's surface

Height above the Earth's surface (meters)	The ether drift velocity (m/sec)			
	This work 2001-2002 Optics	The experiment [13] 1998-1999 Radio waves band	The experiment [79] 1925-1926 Optics	The experiment [10] 1929 Optics
1830	–	–	10000	6000
265	–	–	3000	–
42	–	1414	–	–
4.75	435	–	–	–
1.6	205	–	–	–

It can be seen from the Fig. 9, that different experiment results are near one straight line and in height band from 1.6 m up to 1830 m the ether drift velocity increases with the height growth above the Earth's surface. The boundary layer has considerable thickness, that can be the consequence of the ether stream and atmosphere interaction. These data do not contradict the imaginations of the model [4-6] about the viscous ether and its stream near the Earth's surface. From the table 2, Fig. 8a and the Fig. 9 it can be seen, that the ether drift velocity is rather small near the Earth's surface, that can explain the reason of "zero results" of many experimental works, in which the value 30 km/sec was taken as the ether drift anticipated velocity. In such experiments the metering device sensitiveness was obviously poor. With the expression (1) it can be calculated, that at the ether drift velocity 200-400 m/sec, the methods of the second order almost are inapplicable for measurements, as in this case such methods sensitiveness to the ether drift velocity is low in 6 orders (!) than the sensitiveness of the first order methods.

The ether kinematic viscosity has been measured in the work. The measurement results are explained above in the part "Result analysis of the interferometer tests," that is stipulated by the peculiarities of the experiment implementation. The measured values of the ether kinematic viscosity are in the limits $v_{ea} \approx (5.5 \ldots 7.1) \cdot 10^{-5}$ m^2sec^{-1}. The mean value is equal $v_{ea} = 6.24 \cdot 10^{-5}$ m^2sec^{-1}, that according to the value order coincides with the ether kinematic viscosity value calculated above $v_c \leq 7.06 \cdot 10^{-5}$ m^2sec^{-1}.

Hence, the differences between the dependencies $W_h(S)$ and the ether drift velocity measured values available can be explained by the measurement method differences of the work and the experiments [1-3], [7-9], [10] and differences between arranging heights of measuring systems. The results of four experiments do not contradict each other, that illustrate the reproduced measurement nature of the ether drift effects in various experiments performed in different geographic conditions with different measurement methods applying.
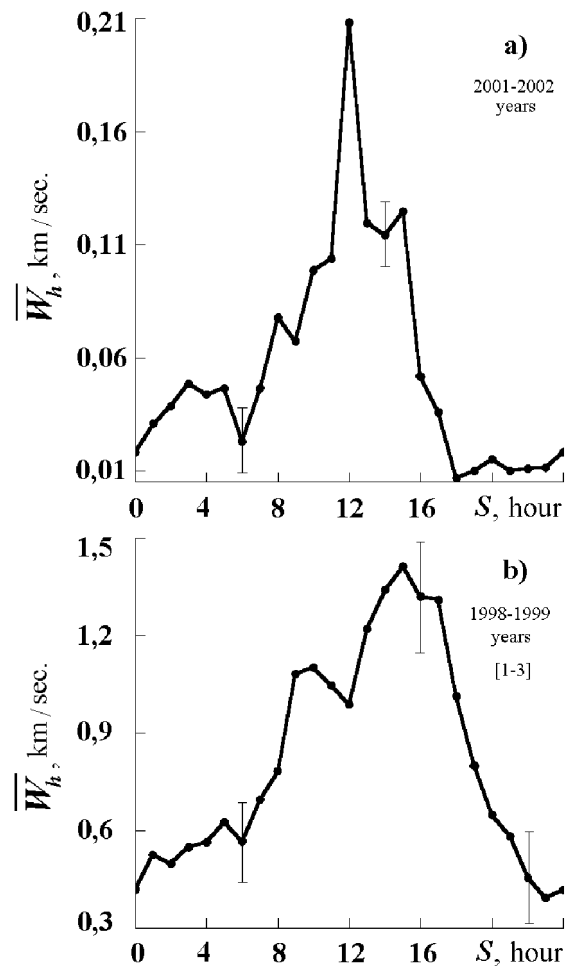
Figure 10: The mean daily course of the ether drift velocity

According to the original hypothesis, the ether drift velocity horizontal component W_h should change its value with the period per one stellar day (the space effect). For revealing the ether drift velocity component with such period, the results of systematic measurements were subjected to statistical processing in stellar time scale. The results of such processing are shown in the Fig. 10. On the fragments of the Fig. 10 the stellar time S in hours is suspended on the abscissa axes, the ether drift velocity value W_h in km/sec is suspended on the ordinate axes. The vertical hatches indicate the confidence intervals. In the Fig. 10a the mean daily course of the ether drift velocity within a stellar day $\overline{W_h\,(S)}$ is given. This dependence is calculated according to the measurement results of the work, which were performed during five months of the year, since September 2001 till January 2002. During five months the numerical value of stellar time shifts regarding to the solar time in 10 hours. Since September till November the measurements were performed on the point No2. In December and January — on the point No3. The mean values are calculated with the expression (43). For comparison, in the Fig. 10b the mean result is given, which was obtained in the experiment [1-3] during year's five months of the same name, since September 1998 till January 1999 (Here, as contrasted to the similar figure, given in the works [1-3], the measured value is expressed in the ether drift velocity values.) In the works [7-9], [10] such data miss, owing to smaller on coverage of year's epochs of the measurement statistics in these experiments.

Both fragments of the Fig. 10 as a whole have similar nature of the ether drift velocity variation within a day. The differences in the curve shapes can be explained by viscous ether stream interaction with the terrain relief elements, which in these different experiments had the distinguished performances and features of radio-frequency spectral line arranging on terrain in the experiment [1-3]. On the fragment of the Fig. 10a (this work), as contrasted to the result of the experiment [1-3] (Fig. 10b), the ether drift velocities have smaller values, that can be explained by the height distinction of measuring points in these experiments. The dependencies $\overline{W_h\,(S)}$ have the forms of periodically changed values with the periods equal to a stellar day, that can be explained by a space (galactic) origin of the ether drift. In the work, the observed bands offset direction of an interference pattern corresponded to the ether drift northern direction at measurement implementation. Hence, the results of the work do not contradict the experiment results [1-3], [7-9], [10] and imaginations of the works [4-6] about the northern position of the ether drift apex, that demonstrate the reproduced result nature of the ether drift effects measurement in different experiments, performed with different measuring methods application.

In the work we shall be confined to qualitative comparison of the work results with the experiment data [1-3], [7-9], [10]. For conducting of quantitative comparative analysis it is necessary to specify the ether drift apex coordinate values on the celestial sphere, which for the first time were determined in the experiment [7-9], to specify an analytical view of the ether drift velocity dependence on the height above the Earth's surface proposed in the works [1-3], to elaborate the calculation method of the terrain relief influence on the ether streams forming near the Earth's surface, to determine probable influencing of the Earth magnetosphere and ionosphere, that is the subject of separate investigations and goes out the frame of the work problems. Due to the reason this experiment results, the experiment [1-3] and the experiment [7-9] are given without any correction, though its usefulness at the result comparison of different experiments is quite obvious.

Thus, in the work, the hypothesis experimental verification about the ether existence in nature, i.e. material medium, responsible for electromagnetic waves propagation, in the optical wave band has been performed. The estimation of the ether kinematic viscosity value has been performed. The first order optical method for the ether drift velocity and the ether kinematic viscosity measuring has been proposed and realized. The method action is based on the development regularities of viscous liquid or gas streams in the directing systems. The significant measurement results have been obtained statistically. The development of the ether drift required effects has been shown. The measured value of the ether kinematic viscosity on the value order has coincided with its calculated value. The velocity of optical wave propagation depends on the radiation direction and increases with height growth above the Earth's surface. The velocity of optical wave propagation changes its value with a period per one stellar day. The detected effects can be explained by the following:

— optical wave propagation medium available regarding to the Earth's movement;

— optical wave propagation medium has the viscosity, i.e. the feature proper to material mediums composed of separate particles;

— the medium stream of optical wave propagation has got a space (galactic) origin.

The work results comparison to the experiment results, executed earlier in order of the hypothesis verification about the existence of such material medium as the ether in nature, has been performed. The comparison results have shown the reproduced nature of the ether drift effect measurements in various experiments performed in different geographic requirements with different measurement methods application.

The work results can be considered as experimental hypothesis confirmation about the ether existence in nature, i.e. material medium, responsible for electromagnetic waves propagation.

References

[1] Yu. M. Galaev. "Ether-drift effects in the experiments on radio wave propagation." *Radiophysics and electronics*, 2000, Vol. 5, No.1, pp. 119–132. (in Ukraine).

[2] Yu. M. Galaev. "Ether-drift. Experiment in the band of radio wave." Zhukovsky: Petit, 2000, 44 pp. (in Russia).

[3] Yu. M. Galaev. "Etheral wind in experience of millimetric radiowaves propagation." *Spacetime & Substance*, 2001, Vol. 2, No. 5(10), pp. 211–225, http://www.spacetime.narod.ru/0010-pdf.zip.

[4] W. Azjukowski. "Dynamik des Äthers." *Ideen des exakten Wissens.*, Stuttgart, 1974, Nu. 2, s. 48–58.

[5] V.A. Atsukovsky. "The introduction into etherdynamics. Model imaginations of material and field structures on the basis of gas like ether." Moskow, MOIP physics dep., 1980, Dep. in VINITI 12.06.80 No. 2760-80 DEP. (in Russia).

[6] V.A. Atsukovsky. "General ether-dynamics. Simulation of the matter structures and fields on the basis of the ideas about the gas-like ether." Energoatomizdat, Moscow, 1990, 280 pp. (in Russia).

[7] D.C. Miller. "Ether drift experiments at Mount Wilson solar observatory." *Phys. Rev.*, 1922, Vol. 19, pp. 407–408.

[8] D.C. Miller. "Ether drift experiment at Mount Wilson." *Proc. Nat. Acad. Amer.*, 1925, Vol. 11, pp. 306–314.

[9] D.C. Miller. "Significance of the ether-drift experiments of 1925 at Mount Wilson." *Science.*, 1926, Vol. 68, No. 1635, pp. 433–443.

[10] A.A. Michelson, F.G. Pease, F. Pearson. "Repetition of the Michelson-Morley experiment." *Journal of the Optical Society of America and Review of Scientific Instruments.*, 1929, Vol. 18, No. 3, pp. 181–182.

[11] E.T. Whittaker. "A History of the Theories of Aether and Electricity." Izhevsk: RIC Regular and random dynamics, 2001, 512 pp. (in Russia). E.T. Whittaker. "A History of the Theories of Aether and Electricity." Thomas Nelson and Sons Ltd, Edinburgh, 1953.

[12] A.A. Michelson. "The relative motion of the Earth and the Luminiferous ether." *The American Journal of Science.*, 1881, III series, Vol. 22, No. 128, pp.120–129.

[13] G.G. Petrash, S.G. Rautian. "Michelson's Interferometer." In the book "Physical encyclopaedic vocabulary." The Soviet encyclopedia, Moskow, 1962, Vol. 2, pp. 202–203 (in Russia).

[14] A.A. Michelson, E.W. Morley. "The relative motion of the Earth and the luminiferous aether." *The American Journal of Science. Third Series.*, 1887, Vol. 34, pp. 333–345; *Philosophical journal.*, 1887, Vol. 24, pp. 449–463.

[15] W.I. Frankfurt, A.M. Frank. "Optics of moving media." Nauka, Moskow, 1972, 212 pp. (in Russia).

[16] S.I. Vavilov. "New searchs of "the ether drift"." *Successes of physical sciences*, 1926, Vol. 6, pp. 242–254 (in Russia).

[17] R.J. Kennedy. "A refinement of the Michelson-Morley experiment." *Proc. Nat. Acad. Sci. of USA.*, 1926, Vol. 12, pp. 621–629.

[18] K.K. Illingworth. "A repetition of the Michelson-Morley experiment using Kennedy's refinement." *Physical Review.*, 1927, Vol. 30, pp. 692–696.

[19] E. Stahel. "Das Michelson-Experiment, ausgefurt im Freiballon." "Die Naturwissenschaften," Heft 41, 1926, B8, Nu. 10, S. 935–936.

[20] Joos G. Die Jenaer. "Widerholung des Mihelsonversuchs." *Ann. Phys.*, 1930, B7, S. 385–407.

[21] "Ether-drift," Digest by Dr. in Sc. V.A. Atsukovsky. Energoatomizdat, Moskow, 1993, 289 pp. (in Russia).

[22] D.C. Miller. "The ether-drift experiment and the determination of the absolute motion of the Earth." *Rev. Modern. Phys.*, 1933, Vol. 5, No. 3, pp. 203–242.

[23] L. Essen. "A new ether drift experiment." *Nature.*, 1955, Vol. 175, pp. 793–794.

[24] J.P. Cedarholm, G.F. Bland, B.L. Havens, C.H. Townes. "New experimental test of special relativity." *Phys. Rev. Letters.*, 1958, Vol. 1, No. 9. pp. 342–349.

[25] D.C. Cyampney, G.P. Isaac, M. Khan. "An ether drift experiment based on the Mssbauer effect." *Phys., Letters.*, 1963, Vol. 7, pp. 241–243.

[26] T.S. Jaseja, A. Javan, J. Murbeam, C.H. Townes. "Test of special relativity or space isotropy by use of infrared masers." *Phys. Rev.*, 1964. Vol. 133a, pp. 1221–1225.

[27] L.G. Loytsyansky. "Mechanics of fluid and gas." Nauka, Moskow, 1973, 848 pp. (in Russia).

[28] N.A. Slezkin. "Dynamics of viscous incompressible fluid." Gostechizdat, Moskow, 1955, 520 pp. (in Russia).

[29] S.G. Rautian. "Rozhdestvensky's Interferometer." In the book "Physical encyclopaedic vocabulary." The Soviet encyclopedia, Moskow, 1962, Vol. 2. p. 203 (in Russia).

[30] L.Z. Rumshisky. "Mathematical processing of the experiment results." Nauka, Moskow, 1971, 192 pp. (in Russia).

ON THE BASIS FOR GENERAL RELATIVITY THEORY

S.N. Arteha[1]

Space Research Institute, Profsoyuznaya 84/32, Moscow 117997, Russia

The basic concepts of the general relativity theory (GRT), such as space, time, the relativity of simultaneity, are systematically analyzed. The logical inconsistencies of basic GRT notions are indicated. Many disputable and contradictory points of this theory and its corollaries are considered in detail.

1. Introduction

A series of logical paradoxes has been analyzed in detail in [1-3], and the complete experimental and logical groundlessness of SRT was demonstrated. Unlike SRT, the GRT contains some rather interesting ideas, such as the principle of equivalence expressed via the idea of "geometrization." If it's basis were true, the GRT could have a claim on status of a hypothesis about some correction to the static Newton's law of gravitation. Since it is not the case, the gravitation theory must be constructed in a different manner.

The basic purpose of this work is the criticism of basis notions of GRT; it is contained in Section 2. A logical inconsistency of space and time notions in GRT is demonstrated here. The plausible errors and disputable points from the textbooks [4-6] are displayed step by step. The time synchronization issues and the Mach principle are also discussed, and the attention is given to doubtful corollaries from GRT. Section 3 contains the conclusions.

2. Criticism of GRT Fundamentals

Many GRT inconsistencies are well-known: 1) the principle of correspondence is violated (the limiting transition to the case without gravitation can not exist without introducing the artificial external conditions); 2) the conservation laws are absent; 3) the relativity of accelerations contradicts the experimental facts (rotating liquids under space conditions have the shape of ellipsoids, whereas non-rotating ones - the spherical shape); 4) the singular solutions exist. (Usually, any theory is considered to be inapplicable in similar cases, but GRT for saving its "universal character" begins to construct fantastic pictures, such as black holes, Big Bang, etc.).

Let us consider the general claims of the GRT. We begin with the myth "on the covariance." The unambiguous solution of any differential equation is determined, except the form of the equation, also by specification of the initial and/or boundary conditions. If they are not specified, then, in the general case, the covariance either does not determine anything, or, at changing the character of the solution, can even result in a physical nonsense. If, however, the initial and/or boundary conditions are specified, then with substitution of the solutions we obtain the identities, which will remain to be identities in any case for any correct transformations. For any solution it is possible to invent the equations, which will be invariant with respect to some specified transformation, if we properly interchange the initial and/or boundary conditions.

The analogies with subspaces are often used in the GRT; for example, a rolled flat sheet is considered. However, the subspace cannot be considered separately from the space as a whole. For example, in rolling a sheet into a cylinder the researcher usually transfers, for convenience, into the cylindrical coordinate system. However, this mathematical manipulation does not influence at all the real three-dimensional space and the real shortest distance.

The simplicity of postulates and their minimum quantity do not still guarantee the correctness of the solution: even the proof of equivalence of GRT solutions is a difficult problem. The number of prerequisites should be, on one hand, sufficient for obtaining a correct unambiguous solution, and, on the other hand, it should provide wide possibilities for choosing mathematical methods of solution and comparison (the mathematics possesses its own laws). The GRT, along with artificial complication of mathematical procedures, has introduced, in fact, the additional number of "hidden fitting parameters" (from metrical tensor components). Since the real field and metrics are unknown in GRT and are subject to determination, the result is simply fitted to necessary one with using a small amount of really various experimental data.

Whereas in SRT though an attempt was made to

---

[1] e-mail: sergey.arteha@mtu-net.ru

confirm the constancy of light speed experimentally and to prove the equality of intervals theoretically, in GRT even such attempts have not been undertaken. Since in GRT the integral $\int_a^b dl$ is not meaningful in the general case, since it can depend on the path of integration, all integral quantities and integral-involving derivations can have no sense.

A lot of questions cause us to muse. If the general covariance of equations is indispensable and unambiguous, then what could be the limiting transition to classical equations, which are not generally covariant? What is the sense of gravitation waves, if the notion of energy and its density is not defined in GRT? Similarly, what is meant in this case by the group velocity of light (and by the finiteness of a signal transmission rate)?

The generality of conservation laws does not depend on the method of their derivation (either by means of transformations from the physical laws or from symmetries of the theory). The obtaining of integral quantities and the use of integration over the surface can lead to different results in the case of motion of the surface (for example, it can depend on the order of limiting transitions). The absence in GRT of the laws of conservation of energy, momentum, angular momentum and center of masses, which have been confirmed by numerous experiments and have "worked" for centuries, cause serious doubts in GRT (following the principle of continuity and eligibility of the progress of science). The GRT, however, has not yet built up a reputation for itself in anything till now, except globalistic claims on the principally unverifiable, by experiments, evolution of the Universe and some rather doubtful fittings under a scarce experimental base. The following fact causes even more doubt in GRT: for the same system (and only of "insular" type) some similarity of the notion of energy can sometimes be introduced with using Killing's vector. However, only linear coordinates should be used in this case, but not polar ones, for example. The auxiliary mathematical means can not influence, of course, the essence of the same physical quantity. And, finally, the non-localizability of energy and the possibility of its spontaneous non-conservation even in the Universe scales (this is a barefaced "perpetuum mobile") cause us to refuse from GRT completely and either to revise the conception "from zero," or to use some other developing approaches. Now we shall pass from general comments to more specific issues.

The question on the change of space geometry in GRT is fully aberrant. The finiteness of the rate of transmission of interactions can change only physical, but not mathematical laws. Whether shall we assert, that the straight line does not exist, only because its drawing into infinity, even at light speed, will require infinite time? (The same is true for the plane and space). The mathematical sense of derivatives can not change as well. One of GRT demonstrations "on the inevitabili-

ty of the change of geometry in the non-inertial system" is as follow: in the rotating coordinate system, due to contraction of lengths, the ratio of the length of a circle to its diameter will be lower, than π. In fact, however, not only the true, but even the observed geometry will not change: whether the <u>mathematical</u> line will move or change as we move? Suppose at first, that the circle will move radially. Let we have three concentric circles of almost the same radius. We place the observers on these circles and number them in the order from the center: 1, 2, 3. Let the second observer be motionless, whereas first and third ones are rotating around center O clockwise and counter-clockwise at the same angular velocity. Then, owing to the difference in relative velocities and contraction of lengths, the observers will interchange their places. However, when they happen to be at the same point of space, they will see different pictures. Indeed, the 1-st observer will see the following position from the center: 3, 2, 1, whereas the 2-nd observer will see the different order: 1, 3, 2, and only the 3-rd observer will see the original picture: 1, 2, 3. So, we have a contradiction. Suppose now, that the geometry of a rotating <u>plane</u> has changed. However, what will be more preferable in such a case: the top or the bottom? The problem is symmetric, in fact; to what side the plane has curved in such a case? If we make the last supposition, that the radius has curved (as the apparent motion changes in the non-inertial system), then the second observer will see it as non-curved, whereas the first and third observers will consider it as "curved" to different sides. Thus, three observers will see different pictures at the same point for the same space; therefore, the curvature of the radius is not an objective fact.

The rotating circle proves the contradictive nature of SRT and GRT ideas. Really, according to the textbooks, the radius, which is perpendicular to the motion, does not change. Therefore, the circles will remain at their places irrespective of the motion. Let us seat the observers on a motionless circle at equal distances from each other and produce a point-like flash from the center of a circle, in order the observers to draw the strokes on moving circles. Owing to the symmetry of a problem, the strokes will also be equidistant. At subsequent periodic flashes each observer will confirm, that a stroke mark passes by him at the flash instant, that is, the lengths of segments of motionless and rotating circles are equal. When the circles stop, the marks will remain at their places. The number of equidistant marks will not change. Therefore, the lengths of segments will be equal in the motionless case as well. Thus, no contraction of lengths and change of geometry took place at all.

Now we consider again the space geometry problem. This problem is entirely confused still since the times of Gauss, who wanted to determine the geometry with the help of light beams. The limited nature of any experi-
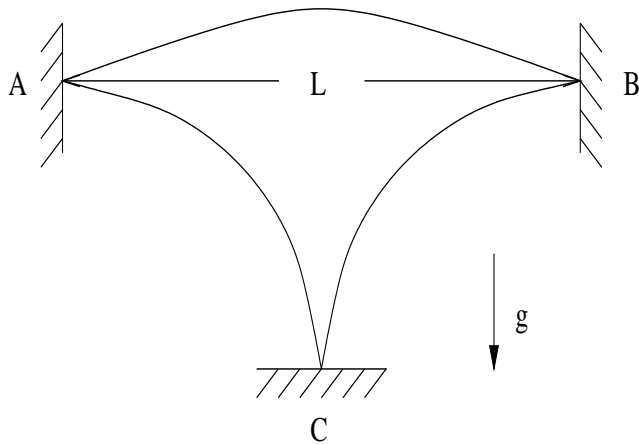
Figure 1: "Geometry of a triangle"

ment can not influence the ideal mathematical notions, does it? Note, that in GRT the light even moves not along the shortest path: instead of Fermat's principle $\delta \int dl = 0$, we have in GRT [4]: $\delta \int (1/\sqrt{g_{00}})dl = 0$, where $g_{\alpha\beta}$ is metric tensor. What does distinguish the light in such a case? The necessity of changing the geometry is often "substantiated" in textbooks as follows: in order the light to "draw" a closed triangle in the gravitational field, the mirrors should be turned around at some angle; as a result, the sum of angles of a triangle will differ from π. However, for any point-like body and three reflectors in the field of gravity (see Fig. 2) the sum of "angles" can be written as:

$$\sum \beta_i = \pi + 4\arctan\left(\frac{gL}{2v_0^2}\right) - 2\arctan\left(\frac{gL}{v_0^2}\right).$$

It occurs, that the geometry of one and the same space depends on the conditions of the experiment: on L and v_0. Since the angle α between the mirrors A and B can also be changed, we have a possibility of artificial changing the geometry within wide limits. Note, that the same variable parameters α and L remain for the light as well. In such "plausible" proofs of the necessity of changing the geometry some important points are not emphasized. First, both in the experiment with material points, and in the experiment with the light the geometry is "drawn" sequentially during some time, rather than instantaneously. Second, for accelerated systems the particles (and the light) move in vacuum rectilinearly, according to the law of inertia, and, actually, the motion of the boundaries of this accelerated system is imposed on this motion additively. All angles of incidence (in the laboratory system) are equal to corresponding angles of reflection, and the "geometry of angles" does not change at all. Simply, the figure is obtained unclosed because of motion of the boundaries. Third, the role of the boundaries is not uncovered at all in determining the relations between the lengths

of real bodies. For example, if all points of a real body are subject to the effect of identical accelerating force, then the mutual relation between lengths and angles ("the geometry") remains unchanged. If, however, only the boundaries are subject to acceleration, then all real changes of bodies' size take place only at interaction with the boundaries. In any case the Euclidean straight lines can be drawn. For example, to draw the horizontal straight line in the gravitational field we take two similar long rods. At the middle of the first rod we install a point-like support. As a result of bending of a rod, the upward-convex line is generated. Then we install two point-like supports for the second rod at the level of two lowered ends of the first rod. As a result of bending of the second rod, the downward-convex line is generated. The middle line between these two bonded rods determines the straight line.

Now we shall turn to the next important GRT notion - the equivalence of the gravitational field to some system non-inertiality. In contrast to any non-inertial system, the gravitational field possesses some unique property: all moving objects deflect in it toward a single center. If we generate two light beams between two ideal parallel mirrors and direct them perpendicular to mirrors, then in the inertial system these beams will move parallel to each other for infinitely long time. A similar situation will take place at acceleration in the non-inertial system, if the mirrors are oriented perpendicular to the direction of acceleration. And, on the contrary, in the gravitational field with similar orientation of mirrors the light beams will begin to approach each other. And, if some effect will happen to be measured during the observation, then, owing to a great value of light speed, the existence of namely the gravitational field (rather than the non-inertiality) can also be found. Obviously, the curvature of mirrors should not be taken into consideration, since, along with gravitational forces there exist also the other forces, which can retain the mutual configuration of mirrors. The distinction of a spherical symmetry from planar one can be found for weak gravitational fields as well. The GRT conclusion on the possibility of excluding the gravitational field for some inertial system during the whole observation time is wrong in the general case.

The equivalence principle of the gravitational field and acceleration can be related to one spatial point only, i.e. it is unreal (it leaded to a false result for the light beam deflection, for example). The equivalence principle of the inertial and gravitating mass can be rigorously formulated also for a separate body only (it is unreal for GRT, since GRT involves interdependence of the space-time and all bodies). Because of this, GRT does not physically proceed to any non-relativistic theory at all (but formally mathematically only). All relativistic linear transformations can be related to empty space only, since real bodies (even as reference points) lead to nonlinear properties of the space. Then, phenome-

na differences with changing reference systems must be studied for the same point (in the space and time). But how can two different observers be placed at one point? Therefore, the relativistic approach can possess the approximate model character only (without globality).

It is not any surprising thing, that the same physical value - a mass - can participate in different phenomena: as a measure of inertia (for any acting forces, including the gravitational one) and as a graviting mass (for example, a moving charge produces both electric and magnetic fields). The question on the rigorous equality of inertial and gravitating massess is entirely artificial, since this equality depends on the choice of a numerical value of the gravitational constant γ. For example, expressions (laws) retain the same form in the case of proportionality $m_g = \alpha m_{in}$, but the gravitational constant will be defined as $\gamma' = \alpha^2 \gamma$. It is not necessary to search any mystics and to create pictures of curved space. The substitution of the same value (for the inertial and gravitating mass) is made not only for GRT, but for the Newton's theory of gravitation as well. It is nothing more than an experimental fact.

When one comes to the dependence of a form of equations on space-time properties [7], there exists some speculation for this idea. The impression is given that we can change this space-time to check the dependence claimed. In fact, the Universe is only one (unique). GRT tries to add a complexity of the Universe to any local phenomena, which is not positive for science. The choice of local coordinates is a different matter (a phenomenon symmetry can simplify the description) and globality is not the case again.

The use of non-inertial systems in GRT is contradictory intrinsically. Really, in a rotating system rather distant objects will move at velocity greater than light speed; but SRT and GTR assert, that the apparent velocities should be lower, than c. However, the experimental fact is as follows: the photograph of the sky, taken from the rotating Earth, indicates, that the visible solid-state rotation is observed. The use of a rotating system does not contradict the classical physics at any distance from the center, whereas in GRT the value of g_{00} component becomes negative (but this is inadmissible in GRT).

The notion of time in GRT is confused beyond the limit as well. What does it mean by the clock synchronization, if it is possible only along the unclosed lines? The change of time reference point in moving around a closed path is an obvious contradiction of GRT, since at a great synchronization rate many similar passes-around can be made, and arbitrary aging or rejuvenation can be obtained. For example, considering the vacuum (emptiness) to be rotating (if we ourselves shall move around a circle), we can get various results depending on a mental idea.

Using the modified paradox of twins [1], the independence of time on acceleration can easily be proven.

Let two astronauts - the twins - are at a great distance from each other. On a signal of the beacon, situated at the middle, these astronauts begin to fly toward a beacon at the same acceleration. Since in GRT the time depends on the acceleration and the acceleration has relative character, each of the astronauts will believe, that his twin brother is younger than he is. At meeting near the beacon they can exchange photos. However, owing to the problem symmetry, the result is obvious: the time in an accelerated system flows at the same rate, as in non-accelerated one. If we suppose the gravitational field to be equivalent to the acceleration (according to GRT), then we obtain, that the time intervals do not depend on the gravitational field presence.

Now we make some remarks concerning the method of synchronization of times by means of a remote periodic source disposed perpendicular to the motion of a body [1]. We begin with inertial systems. The possibility of time synchronization on restricted segments makes it possible to synchronize the time throughout the line of motion. Indeed, if for each segment there exists an arbitrarily remote periodic source sending the following information: its number N_j, the quantity n_j of passed seconds (the time reference point is not coordinated with other sources), then the observers at junctions of segments can compare the time reference point for a source on the left and for a source on the right. Transmitting this information sequentially from the first observer to the last one, it is possible to establish a single time reference point (the time itself, as it was shown in [1], has absolute sense).

Apparently, the observed rate of transmission of synchronization signals has no effect on the determination of duration of times: the pulses (for example, light spheres or particles), which mark the number of passed seconds, will equidistantly fill the whole space, and the number of spheres emitted by a source will be equal to the number of spheres, which intersect the receiving observer. (We are not the gods, you see, to be able to introduce the "beginning of times": the time takes already its normal course and elapses uniformly.) Even if we consider the apparent signal propagation rate to be $c = c(\mathbf{r})$, then, irrespective of the path of light, the number of spheres reached the receiving observer (having a zero velocity component in the source direction) will be the same as the number of spheres emitted by a source (simply, the spheres can be spatially thickened or rarefied somewhere). Thus, the full synchronization is possible in the presence of spatial inhomogeneities (of the gravitational field) as well.

In physics it is not accepted to take into account the same effect twice. It is clear, that the acceleration and gravitation express some force, that influences various processes. But this will be the general result of the effect of namely the forces. For example, not any load can be withstood by a man, the pendulum clock will not operate under zero gravity, but this does

not mean, that the time stopped. Therefore, the rough Hafele-Keating's experiment states the trivial fact, that the gravitation and acceleration somehow influence the processes in a cesium atomic watch, and the high relative accuracy of this watch is fully groundless for a fixed site. Besides, interpretation of this experiment contradicts the "explanation" of the Pound-Rebka's experiment with supposition about independence of frequency of emission in "the units of intrinsic atom time" [5] on gravitational field. Besides, a further uncertainty in GRT must be taken into consideration: there can exist immeasurable rapid field fluctuations (with a rate greater than inertness of measuring instruments) even in the absence of the mean field $\mathbf{g}$. Such the uncertainty exists for any value of $\mathbf{g}$: since the time in GRT does not depend on $\mathbf{g}$-direction, then an effective potential will be nonzero even with $< \mathbf{g} >= 0$. Whether is it possible to invent, though theoretically, a precise watch, which can be worn by anybody? Probably, a rotating flywheel with a mark (in the absence of friction - on a superconducting suspension), whose axis is directed along the gravitational field gradient (or along the resultant force) could read out the correct time. At least, no obvious reasons and mechanisms of changing the rotation rate are seen in this case. Certainly, for weak gravitation fields such a watch will be less accurate at the modern stage, than cesium one. We hypothesize, that atom decay is anisotropic, and this anisotropy can be interrelated with a direction of the atomic magnetic moment. In this case we can regulate atomic moments and freeze the system. Then, the "frozen clock" will register different time depending on its orientation in the gravitational field.

Now we return to synchronizing signals (for simultaneous measurement of lengths, for example). For a rectilinearly moving, accelerated system it is possible to use the signals from a remote source being perpendicular to the line of motion, and for the segment of a circle the source can be at its center. These cases actually cover all non-inertial motions without gravitation. (Besides, for the arbitrary planar motion it is possible to make use of a remote periodic source being on a perpendicular to the plane of motion.) For the real gravitational field of spherical bodies in arbitrary motion along the equipotential surfaces it is possible to use periodic signals issuing from the gravitational field center.

Note, that to prove the inconsistency of SRT and GRT conclusions on the change of lengths and time intervals it is sufficient, that the accuracy of ideal measurement of these values could principally exceed the value of the effect predicted by SRT and GRT. For example, for a source being at the middle perpendicular to the line of motion we have: $\Delta t = l^2/(8Rc)$; that is, Δt can be decreased not only by choosing the great radius of a light sphere, but also by choosing a small section of motion l. From the SRT formulas on time

contraction we have: $\Delta t = l(1 - \sqrt{1 - v^2/c^2})/v$. If for finite R and specified speed v we choose such l, that the inequality

$$l/(8Rc) < (1 - \sqrt{1 - v^2/c^2})/v, \qquad (1)$$

be met, then the conclusions of relativistic theories occur to be invalid.

For the system arbitrarily moving along the radius (drawn from the gravitational field center) it is possible to use for synchronization a free falling periodic source on the perpendicular to the line of motion. In this case R should be chosen of such value, that the field can not actually change (due to equipotential sphere rounding) at this distance, and corresponding l from (1) near the point, to which the perpendicular is drawn. Therefore, the GRT conclusions can be refuted in this case as well. For the most important special cases the "universal" SRT and GRT conclusions on the contraction of distances as a property of the space itself are invalid. In the most general case it seems intuitively quite obvious, that such a position of a periodic source can be found, that the signal to come perpendicular to the motion, and that such R and l from (1) to exist, which refute the GRT results. There is no necessity at all in a "spread" frame of reference and in an arbitrarily operating clock: any change of real lengths should be explained by real forces; it is always possible to introduce a system of mutually motionless bodies and the universal time. Thus, the space and time must be Newtonian and independent on the motion of a system.

Now we pass to mathematical methods of GRT and to corollaries of this theory. The games with the space-time properties result in the fact, that in GRT the application of variation methods occurs to be questionable: the quantities are not additive, the Lorentz transformations are non-commutative, the integral quantities depend on the path of integration. Even it is not clear, how the terminal points can be considered as fixed, if the distances are different in different frames of reference.

Because of nonlocalizableness (non-shieldness) of gravitation field, conditions on infinity (because of the mass absence on infinity, it is euclideanness) are principally important for the existence of the conservation laws [7] (for systems of the insular type only). The classical approach is more successive and useful (theoretically and practically): energy is determined correctly to a constant, since the local energy difference between two transition points has a physical meaning (therefore, conditions on infinity is groundless).

Highly doubtful is the procedure of linearization in the general form, since it can be only individual. The tending to simplicity is declared, but even two times are introduced - coordinate and intrinsic ones. The fitting to the well-known or intuitive (classically) result is often made. So, for motion of Mercury's perihelion [5] the $du/d\varphi$ derivative can have two signs. Which

of them should be chosen? To say already nothing of the fact, that the dividing by $du/d\varphi$ is performed, but this quantity can be zero. Calculating the perihelion displacement in GRT (from the rigorous solution for a single attractive point), the impression is given that we know astronomical masses exactly. If we use GRT as a correction to Newton's theory, the situation is in fact opposite: there exists a problem knowing visible planet motions to reestablish the exact planet masses (to substitute the latters and to check GRT thereafter). Imagine the circular planet orbit. It is obvious in this case, that the Newtonian rotation period will already be taken with regard to an invisible precession, i.e. the period will be renormalized. Therefore, renormalized masses are already included in Newton's gravitation theory. Since the GRT-corrections are much less than the perturbation planet actions and the influence of a non-sphericity, the reestablishment of exact masses can essentially change the description of a picture of the motion for this complex many-body problem (see other objections [2]). No such detailed analysis was carried out. The complexity of spatial-temporal links is stated, but eventually one passes for a very long time to customary mathematical coordinates; otherwise there is nothing to compare the results with. For what was there a scrambling?

The prototype of the "black hole" in Laplac's solution, where the light, moving parallel to the surface, begins to move over a circle like the artificial satellite of the Earth, differs from the GRT ideas. Nothing prohibits the light with a rather high energy to escape the body in the direction perpendicular to its surface. There is no doubt, that such beams will exist (both by internal and external reasons): for example, the beams falling from outside will be able to accumulate energy, in accordance with the energy conservation law, and to leave such a "black hole" after reflecting. "The black holes" in GRT is a real mysticism. If we take a long rod, then at motion its mass will increase and the size will decrease (according to SRT). What will happen? Is "the black hole" generated? All the sky will become filled with "black holes," if we shall move rapidly enough. And, you see, this process would be irreversible.

The presence of singularities or multiple connection of the solution implies, that, as a minimum, the solution is inapplicable in these regions. Such a situation takes place with the change of the space - time signature for the "black hole" in the Schwarzschild solution, and it is not necessary to search any artificial philosophical sense in this situation. The singuliarity in the Schwarzschild solution for $r = r_g$ cannot be eliminated by purely mathematical manipulations: the addition of the infinity with the other sign at this point is the artificial game with the infinities, but such a procedure requires the physical basis. (You see, the singularity at zero is not eliminated by artificial addition of $\alpha \exp(-\lambda r)/r$,

where λ is a large quantity).

Even from GRT follows the impossibility of observation of "black holes": the time of "the black hole" formation will be infinite for us as remote observers. And since the collapse cannot be completed, the solutions, which consider all things as though they have already happened, have no sense. The separation of events by infinite time for internal and external observers is not "an extreme example of the relativity of the time course," but the elementary manifestation of the inconsistency of Schwarzschild's solution. The same fact follows from "the incompleteness" of systems of solutions. It is not clear, what will happen with the charge conservation law, if a greater quantity of charges of the same sign will enter "the black hole"? The mystical description of "metrical tidal forces" [6] at approaching "the black hole" is invalid, since it would mean, that the gravitation force gradient is great within the limits of a body, but all GRT ideas are based on the opposite assumptions. The Kerr metric in the presence of rotation also clearly demonstrates the inconsistency of GRT: it gives in a strict mathematical manner several physically unreal solutions (the same operations, as for Schwarzschild's metric, do not save the situation).

GRT contains a lot of doubtful prerequisites and results. List some of them. For example, the requirement of gravitational field weakness for low velocities is doubtful: if the spacecraft is landed on a massive planet, whether it can not stand or slowly move? Whether some molecules with low velocities cannot be found in spite of temperature fluctuations? The consideration of a centrally symmetric field in GRT has not physical sense as well: since the velocity can be only radial, then not only rotations, but even real temperature characteristics can not exist (i.e. $T = 0K$). The field in a cavity is not obtained in a single manner, but, simply, two various constants are postulated in order to avoid singularities. The emission of gravitation waves for a parabolic motion (with eccentricity $e = 1$) results in the infinite loss of energy and angular momentum, which obviously contradicts the experimental data. In fact, GRT can be applied only for weak fields and weak rotations, i.e. in the same region, as the Newtonian theory of gravitation. Recall that the interaction between moving charges differs from the static Coulomb law. Therefore, prior to applying the static Newtonian law of gravitation, it must be verified for moving bodies, but this is a prerogative of the experiment.

The theories of evolution of the Universe will remain the hypotheses for ever, because none of assumptions (even on the isotropy and homogeneity) can be verified: "a moving train, which departed long ago, can be catched up only at the other place and at the other time." GRT assigns to itself the resolution of a series of paradoxes (gravitational, photometric, etc.). However, the classical physics has also described the possibilities of resolution of similar paradoxes (for example, by

means of Charlier's structures, etc.). Apparently, the Universe is not a spread medium, and we do not know at all its structure as a whole to assert the possibility of realization of conditions for similar paradoxes (more probably, the opposite situation is true). For example, the Olbers paradox can easily be understood on the basis of the analogy with the ocean: the light is absorbed, scattered and reflected by portions, and the light simply ceases to penetrate to a particular depth. Certainly, such "a depth" is huge for the rarefied Universe. However, the flashing stars represent rather compact objects spaced at great distances from each other. As a result, only a finite number of stars make a contribution into the light intensity of the night sky.

The expanding of the Universe gives a red shift according to the Doppler effect irrespective of GRT. Besides, it should be taken into consideration, that even the elementary scattering will make contribution into the red shift and filling of the so-called relic radiation: recall that the Compton effect gives waves with $\lambda' > \lambda_0$. The shift of lines in the gravitational field has been well predicted even by mechanistic models from the general energy considerations.

Now we pass to the following principal issue. Whether positive is the fact, that the distribution and motion of the matter cannot be specified arbitrarily? And whether is it correct? Generally, this implies the inconsistency of the theory, because there exist other forces, except gravitational ones, which are also capable to transpose the matter. From the practical viewpoint this means, that we should specify all distributions in "the correct-for-GRT" manner even at the initial time instant. In such a case we should refer t_0 instant to "the time of creation," did we? And what principles should be unambiguously determinate for such a choice? This requires more knowledge, than it is expected from GRT. Open to question occurs to be the possibility of point-like description and the theory of disturbances, because the resulting values cannot be arbitrary as well. The joining of a completely unknown equation of state implies artificial complication of macro- and micro-levels by linkage and reflects the possibility of arbitrary fittings (for example, the temperature dependence is rejected). The possibility of adding the cosmological constant into Einstein's equations is an indirect recognition of ambiguity of GRT equations and of possible outrage. If everything can be specified to such an accuracy, then why cannot we specify in arbitrary manner the initial distribution and the motion of a matter?

Let us discuss one more principal point concerning the relativity of all quantities in GRT. The laws, written simply as the equations, determine nothing by themselves. The solution of any problem still requires the knowledge of specific things, such as the characteristics of a body (mass, shape etc.), the initial and/or boundary conditions, the characteristics of forces (magnitude,

direction, points of application etc.). "The reference points" are actually specified, with respect to which the subsequent changes of quantities (position, velocity, acceleration etc.) are investigated. The principal relativity of all quantities in GRT contradicts the experiments. The subsequent artificial attempt to derive accelerations (or rotations) with respect to the local geodesic inertial Lorentzian system - this is simply the fitting to only workable and experimentally verified coordinates of the absolute space (GRT does not contain any similar things organically [7]).

The Mach principle of stipulation of an inert mass and absolute nature of the acceleration due to the influence of far stars is also doubtful, since it explains the intrinsic properties of one body via the properties of other bodies. Of course, the idea is elegant in itself. If everything in the world is supposed to be interdependent and some ideal complete equation of state is believed to exist, then any property of bodies should be determined by the influence of the whole remaining Universe. However, in such a case any particle should be considered to be individual. This way is faulty for science, which progresses from smaller knowledge to greater, since "it is impossible to grasp the immense." Actually, if we take into account the non-uniform distribution of mass (in compact objects) and different values of attraction forces from close and far objects, then the complete "tugging" would be obtained instead of uniform rotation or uniform inertial motion of an object.

The Mach principle cannot be verified in essence: both removal of all bodies from the Universe and tending of the gravitation constant to zero are the abstractions having nothing in common with the reality. However, it is possible to estimate the influence of "far stars" experimentally by considering the mass of the Universe as mainly concentrated in compact objects. The force of attraction of a star having a mass of the order of the Sun's mass ($M \sim 2 \cdot 10^{30}$ kg), being at the distance of 1 light year ($\sim 9 \cdot 10^{15}$ m), is equivalent to the action of a load having a mass of only $m_0 \sim 25$ g at the distance of 1 meter. We shall make use, for a while, of the doubtful Big Bang theory and shall consider the time for the Universe to be equal to $\sim 2 \cdot 10^{10}$ years. Even if the stars fly away with light speed, we would have the size of the Universe equal to $\sim 2 \cdot 10^{10}$ light years. We have deliberately increased all quantities; for example, the mass of the Universe and its density $\rho \sim 10^{33}/10^{54} \sim 10^{-21}$ g/cm^3. We take into account now, that, as the bodies move away from each other at the two-fold distance, the force decreases four-fold, etc. Even if we suppose the mean distance between the stars to be 1 light year, then at the distance of 1 meter it is necessary to place the mass (we sum up to $2 \cdot 10^{10}$) of $M_0 \sim 25(1 + 1/4 + 1/9 + \cdots) = 25 \sum 1/n^2 \sim 25\pi^2/6 < 50$ g. In fact, coefficient $\pi^2/6$ expresses some effective increase of the density at the observation line. To simulate the action of "the whole Universe" we can
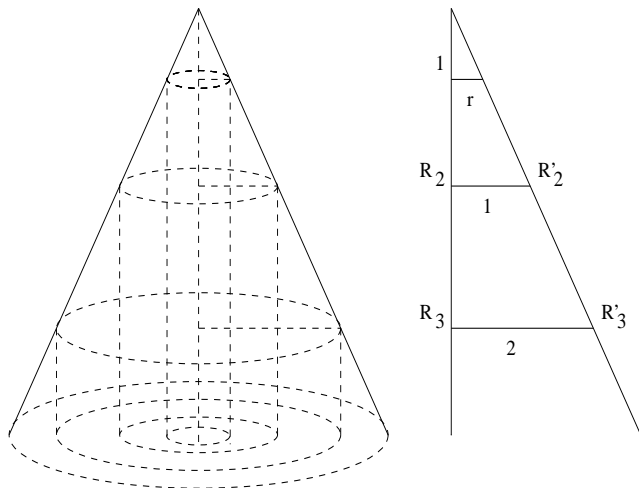
Figure 2: The Mach principle and influence of the Universe

take a thick metal sphere with outer radius of 1 meter and make its thickness varying in the direction to the center.

Let the width of a solid sphere be 0.6 meters, i.e. from the center up to 0.4 meters there is a niche, and further, up to 1 meter, - the metal. Then a cylindrical column of radius ~ 0.35 cm will correspond to mass M_0 at density of ~ 8.3 g/cm^3. In reality, we should take into account the influence of stars in a cone, but not only in a cylinder. Though we also have a spherical metal cone, nevertheless, we shall estimate the orders of magnitudes. We shall break a cone into cylindrical layers, which arise as the new layers of stars are involved into consideration (Fig. 2). Each new layer will be greater, than a preceding layer, by 6 stars. The distances from the center to the nearest boundary of each layer of stars can be found from the similarity of triangles: $R_i/1 = i/r$. Then we have $R_i' = \sqrt{i^2(1+r^2)}/r$. Therefore, the correction to a mass (we sum up to $2 \cdot 10^{10}$) will be found as

$$m_0\left(1 + \frac{1}{4} + \cdots\right)\left(1 + \sum_i \frac{6}{R_i'^2}\right) < M_0\left(1 + 6r^2 \sum_i \frac{1}{i}\right) \sim$$

$$M_0\left(1 + 6 \cdot 10^{-5} \log\left(2 \cdot 10^{10}\right)\right) \sim M_0\left(1 + 0.02\right).$$

Thus, our construction is quite sufficient for taking into account "the whole Universe." Certainly, if the Universe is infinite, then the obtained harmonic series will diverge, and the construction will be inadequate. This, however, contradicts both GRT and the modern ideas.

Let now place the globules on a spring inside the sphere. To avoid the collateral effects, the air can be pumped out from the structure and, in addition, the globules can be isolated from the sphere by a thin vessel. Now, if we spin up the sphere, then, according to the Mach principle, the centrifugal force should appear, and the globules will move apart of each other.

In this case the centrifugal force must be the same, as though the globules themselves would rotate. It seems quite obvious, that this is impossible, since such an effect would be noticed still long ago. Thus, we return to absolute notions of acceleration, mass, space and time defined still by Newton. However, the described experiment could appear to be useful for determining the corrections to the static Newton's law of gravitation. In this case the globules should have sufficient freedom to move and to rotate, since the direction of action of correcting forces and moments of forces is unknown a priori.

The gravitational constant is not a mathematical constant at all, but it can undergo some variations [9]. Therefore, this value can account corrections to Newton's static law of gravitation (for example, these influences do not taken into consideration for the displacement of the perihelion of the Mercury). Generally speaking, the theory of short range for gravitation could be useful (but it can be not useful depending on the gravitation transmission rate) for the finite number of cases only: for the rapid $(v \to c)$ motion of massive (the same order) bodies close to each other. The author does not know such practical examples.

The GRT approach to gravitation is unique: to be shut in the lift (to take pleasure from the fall) and to be not aware that the end (hurt oneself) will be after a moment. Of course, the real state is quite different one: we see always where and how we move relative to the attractive centre (contrary to Taylor and Wheeler, it is the second "particle," together with the first "particle" — with the observer). That is the reason that the pure geometric approach is a temporal zigzag for physics (although it could ever be useful as a auxiliary technique). And two travelers from the parable [10] have need for "very little": for the wish to move from the equator just along meridians (on the spheric earth surface), but the rest of five billion mans can not have such the wish. Contrary to traveler's wish, the wish "to do not attract to the Earth (or the Sun) and to fly away to space" is inadequate. The notion force (the force of gravity in this case) reflects this fact. Geometry cannot answer to the following questions: how many types of interactions exist in nature, why there exist they only, why there exist local masses, charges, particles, why the gravitational force is proportional just to r^2, why there realize the specific values of physical constants in nature, and many other questions. These problems are the physical (experimental) prerogative.

3.   Conclusions

The paper is devoted to the GRT criticism. A set of striking doubtful points from the GRT textbooks is emphasized, beginning with general concepts of the covariance, baseline physical notions, and finishing with more

specific ones. The proof of the geometry invariance in a rotating coordinate system is carried out in detail. The groundlessness and inconsistency of the principle of equivalence in GRT is discussed. The inconsistency of the notion of time and its synchronization in GRT is demonstrated. The methods of time synchronization and simultaneous measurement of lengths are indicated for the most interesting special cases. The invariance of space geometry is demonstrated and the role of boundaries is also discussed in the paper. The doubtful points are emphasized both for the methods and for numerous corollaries of GRT. The inconsistency of the notion of "black holes," of Schwarzschild's solution and other GRT corollaries are considered in detail. The Mach principle and its possible verification are also discussed.

The ultimate conclusion of the paper consists in the necessity of returning to classical notions of space and time and of constructing the gravitation theory on this established basis.

References

[1] S.N. Arteha, "On the Basis for Special Relativity Theory," to be published in *Galilean Electrodynamics*.

[2] S.N. Arteha, "On Frequency-Dependent Light Speed," to be published in *Galilean Electrodynamics*.

[3] S.N. Arteha, "On Relativistic Kinematic Notions," to be published in *Galilean Electrodynamics*.

[4] L.D. Landau and E.M. Lifshitz, "The classical Theory of Fields," Nauka, Moscow, 1988 (in Russian).

[5] P.G. Bergmann, "Introduction to the Theory of Relativity," Inostrannaya Literatura, Moscow, 1947 (in Russian).

[6] E. Schmutzer, "Relativit*ä*tstheorie - Aktuell," Mir, Moscow, 1981 (in Russian).

[7] V. Fock, "The Theory of Space, Time and Gravitation," Pergamon Press, London, 1959.

[8] A.A. Logunov, M.A. Mestvirishvili, "Relativistic Theory of Gravitation," Nauka, Moscow, 1989 (in Russian).

[9] V.P. Ismailov, O.V. Karagios, A.G. Parkhanov, "The Investigation of variations of experimental data for the gravitational constant," *Physical Thought of Russia* **1/2**, 20–26 (1999).

[10] E.F. Taylor, J.A. Wheeler, "Spacetime Physics," W.H. Freeman and Company, San Francisco, 1966.

ANOMALIES IN MOVEMENT OF "PIONEER 10/11" AND THEIR EXPLANATION

N.A. Zhuck[1]

Research and Technological Institute of Transcription, Translation and Replication, JSC
Box 589, 3 Kolomenskaya St., Kharkov 61166, Ukraine

August 17, 2002

The author has offered the version of an explanation of anomalies of the Pioneer 10/11 motion on the basis of the Universe gravitational viscosity.

Pioneer 10 was launched on 2 March 1972 and it functions till now.

Pioneer 10 distance from Sun: 80.68 AU Speed relative to the Sun: 12.24 km/sec (27,380 mph) Distance from Earth: 12.21 billion kilometers (7.59 billion miles) Round-trip Light Time: 22 hours 38 minutes

Launched on 5 April 1973, Pioneer 11 followed its sister ship. Its mission ended on 30 September 1995, when the last transmission from the spacecraft was received.

Pioneer 10/11 have anomalies in the motion. A discussion of this phenomenon appears in the 4 October 1999 issue of Newsweek magazine. The mystery of the tiny unexplained acceleration towards the Sun in the motion of the Pioneer 10, Pioneer 11 and Ulysses spacecraft remains unexplained.

A team of planetary scientists and physicists led by John Anderson has identified a tiny unexplained acceleration towards the Sun in the motion of the Pioneer 10, Pioneer 11, and Ulysses spacecraft. The anomalous acceleration — about 10 billion times smaller than the acceleration we feel from Earth's gravitational pull ($0.76 \cdot 10^{-10}$ m/sec^2 in report [1]) — was identified after detailed analyses of radio data from the spacecraft.

A variety of possible causes were considered including: perturbations from the gravitational attraction of planets and smaller bodies in the Solar system; radiation pressure, the tiny transfer of momentum when photons impact the spacecraft; general relativity; interactions between the Solar wind and the spacecraft; possible corruption to the radio Doppler data; wobbles and other changes in Earth's rotation; outgassing or thermal radiation from the spacecraft; and the possible influence of non-ordinary or dark matter.

After exhausting the list of explanations deemed most plausible, the researchers examined possible modification to the force of gravity as explained by Newton's law with the Sun being the dominant gravitational force.

However in 1984 the author of this work has deduced the new formula of a free motion of a material body instead of the Newton's first law [2]

$$\frac{d^2 X}{dt^2} + H \frac{dX}{dt} = 0, \qquad (1)$$

where the label is entered

$$H = \sqrt{\frac{4\pi G \rho_0}{3}}, \qquad (2)$$

which corresponds to the Hubble constant, but has other physical sense (here ρ_0 is medial density of the Universe; X is a coordinate). It now reflects a dissipation of energy at a motion of material bodies and at spread of fields. The Hubble constant is very small and equal approximately 10^{-18} 1/sec.

Medial density of a substance is equal approximately $4 \cdot 10^{-21}$ kg/m^3 in region of Solar system (one star per 10 cubic kiloparsecs). Then the Hubble parameter will be equal $1.1 \cdot 10^{-15}$ 1/sec. And the acceleration of Pioneer 10 equal $(-1.3) \cdot 10^{-11}$ m/sec^2 for the present time. Earlier acceleration was more.

Thus, the gravitational viscosity is the most probable reason of motion anomaly of the Pioneer 10/11. At least gravitational viscosity should be studied.

References

[1] N.I. Kolosnitsyn. "Relativistic orbit form and anomalies in "Pioneer 10/11" dynamics." Abstracts of 11-th International Conference "Theoretical and experimental problems of General Relativity and gravitation," 2002, pp. 68-69.

[2] N.A. Zhuck. "Gravitation viscosity and geotetic curvature of the Universe." *Spacetime & Substance*, 1, 2, 71–77 (2000). http://spacetime.narod.ru.

[1]e-mail: zhuck@ttr.com.ua

AGAIN ON THE GUALA-VALVERDE HOMOPOLAR-INDUCTION EXPERIMENTS

Ricardo Achilles[1]

Confluencia Tech University, Rosas y Soufal - P. Huincul Neuquen, ARG Q8318EFG

After independent repetition of the recently reported break-through experimentation on homopolar induction by Guala-Valverde et al [Apeiron, **8**, 41 (2001)] some considerations are drawn on the torque-production mechanism applicable to machines founded on that principle. These considerations are based on the "action-at-a-distance" Ampre-Weber-Assis rationale.

1. Introduction

The Guala-Valverde (G-V) and coworkers success in solving the old conundrum known as homopolar induction rests upon the singularity introduced in an uniform magnet [1], [2], [3], [4], [5] providing a local, short range **B**-*field* reversion. The most striking feature of the G-V homopolar-motor experiments occurs when the *probe* is located in the singularity: while the free-to-rotate probe denotes the presence of forces in correspondence with the field reversion observed in that region, the stationary *circuit-closing wire* remains insensitive to the magnet singularity. It behaves as if there were no singularity at all! This experimental fact enabled G-V to locate the seat of electromotive and ponderomotive actions in homopolar machines [1] confirming besides the symmetry of both, generator and motor configurations. The aforementioned, quiet a trivial fact for ordinary flux-varying machines, was a rather obscure issue for almost two centuries in the homopolar devices' case.

Energy conversion by a machine is made possible by the relative motion of two of its constitutive parts; in the specific case of electrical machines these two parts are an active conductor -the probe or the closing wire in G-V's nomenclature- and a magnet (or a second active conductor). Any electrical-circuit part anchored to the magnet will no longer play an active energy-conversion role; it will be just a current-path closing means. The remaining electrical circuit -with motion relative to the magnet enabled- takes over energy conversion (mechanical to electrical for a generator or vice versa for a motor). Fig. 1 sketches a homopolar motor where a centripetal direct current is applied to the probe attached to the upward **B**-*field* face of a disk magnet. The main interaction in this case can be split in two [1], [6]:
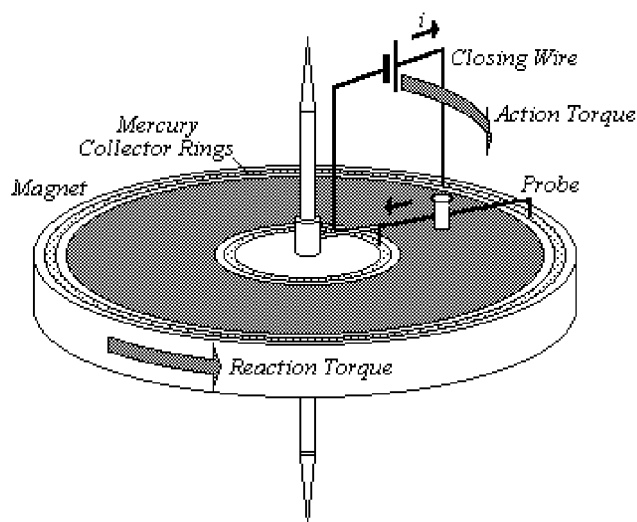
Figure 1: Torques on the homopolar-motor magnet and closing wire

— Magnet-probe: The magnet exerts a counter-clockwise torque on the probe, the probe an equal but opposite torque on the magnet.

— Magnet-closing wire: The magnet exerts a clockwise torque on the closing wire, the closing wire an equal but opposite torque on the magnet.

The probe attached to the magnet does not permit relative motion and the action-reaction cancellation mechanism among both parts inhibits energy conversion. On the contrary, the closing wire -with electrical continuity with the probe attained via the mercury collector rings- possesses relative motion with respect to the magnet enabling energy conversion. This latter interaction is the main responsible for the observed magnet-plus-probe rotation. Ironically, and against the customary absolutist argument of the magnet being dragged by the probe [1], the magnet is the drag-

---

[1] e-mail: achilles@ieee.org

Figure 2: Ampre-law current elements

Figure 3: Magnetizing shell-probe Ampre interaction in the uniform field motor
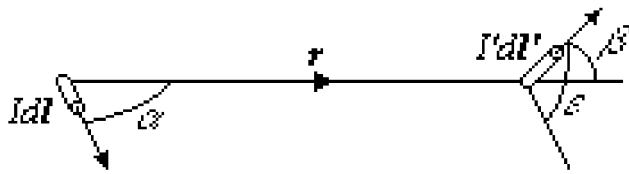
ging agent. The additional closing wire-probe (current-current) interaction was dismissed in the G-V analysis due to its negligible effect in comparison to the described mechanism.

As an IEEE member, last months some specialists came along asking me on the homopolar torque-production mechanism. I am intending to answer on this issue here.

2. Ampre versus Standard Electrodynamics

Ampre force law [7], [8], draws the expression for the magnitude of the mechanical forces applied on two current elements $Id\mathbf{l}$, $I'd\mathbf{l}'$ separated a distance $\mathbf{r}$ (see Fig. 2) as:

$$d^2F = -(\mu_o/4\pi)(I \cdot I'/r^2)[(2(d\mathbf{l} \cdot d\mathbf{l}') -$$

$$-3(\mathbf{r} \cdot d\mathbf{l})(\mathbf{r} \cdot d\mathbf{l}')/r^2]. \qquad (1)$$

This formulation supplies a quite suitable tool to better understand the homopolar phenomena: the $d^2\mathbf{F}$ forces obey Newton's third law being its direction coincidental with the one of the segment $\mathbf{r}$ defining the distance between the current elements. Repulsion (attraction) occurs for a positive (negative) $d^2\mathbf{F}$ magnitude.

As it is well known, a magnet may be modeled by Ampre equivalent magnetizing currents [9], [10]. In the homopolar-motor uniform $\mathbf{B}$-*field* case, the magnet can be defined as a cylindrical azymuthal current shell. The equivalent current I' of such a cilindrical magnet is shown in Fig. 3, in conjunction with a centripetal conduction current I circulating through the probe. A few quantitative considerations based on equation (1) can be applied to the above described configuration to understand the homopolar torque-production mechanism: the Ampre formulation dependence on $(1/r^2)$ defines the magnetic-shell current elements located more closely to the probe as the ones producing the main interaction. Let us consider the action of two such current elements $I'd\mathbf{l}'$ and a probe conduction-current element $Id\mathbf{l}$ (see Fig. 3): an attraction force $d^2\mathbf{F'}_1$ (repulsion force $d^2\mathbf{F'}_2$) will appear on the magnet-shell element $d\mathbf{l}'$ located above (below) the probe element $d\mathbf{l}$. Such forces will include, in the general case indicated in the
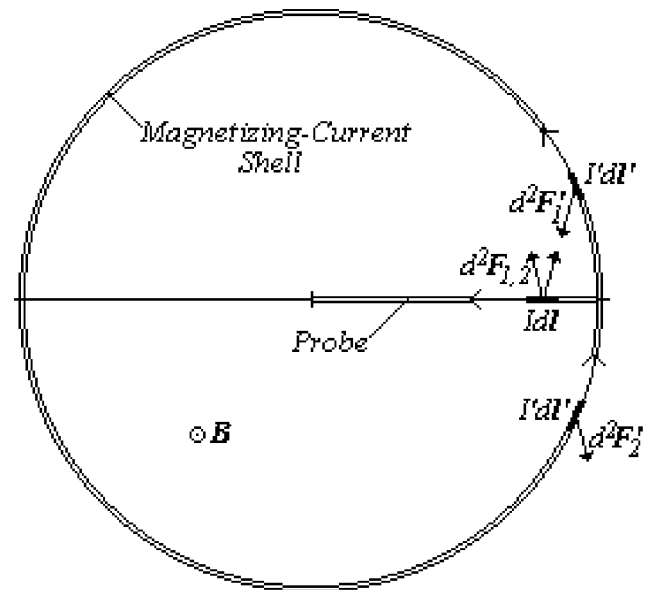
figure, radial and azymuthal components acting on the bulk of the magnet. These latter components are the main responsibles for the observed clockwise rotation. This dominant interaction can be eliminated simply by attaching the probe to the magnet. In such case, the only interaction left is the counterclockwise torque applied on the magnet by the closing-wire current.

Standard Electrodynamics (SE) considerations based on the Laplace's expression $d\mathbf{F} = I(d\mathbf{l}\mathbf{x}\mathbf{B})$ applied to the magnetizing current elements fail to explain homopolar-devices torque production since -by vector product properties- **all** the forces acting on the shell current elements are radial to the magnet and, therefore, unable to generate torque (It has to be kept in mind that during the last century the unrestricted equivalence of the Ampre and SE formulations was confirmed for closed circuits [7]). Moreover, a closed circuit in the vicinity of an arbitrary current element will apply on it forces perpendicular to its length (a fact manifestly observed in the probe). In the G-V experiments the interaction to look at is the one existing between a finite current element (the probe or the closing wire) and a closed circuit (the $\mathbf{B}$-*field* equivalent magnetizing current). And here, according to SE, the closing wire is unable to produce any torque on the magnet: a fact quite in opposition to experience! Conversely, the interaction of the magnet with the mechanically attached probe- plus-closing-wire circuit leads to the same outcome for either formulation: a null torque on both, closed circuit and magnet [7], [11]. At last, it is also interesting to have a look of the current interaction taking place in the magnet's singularity shown in Fig. 4. The currents interacting here are the centripetal
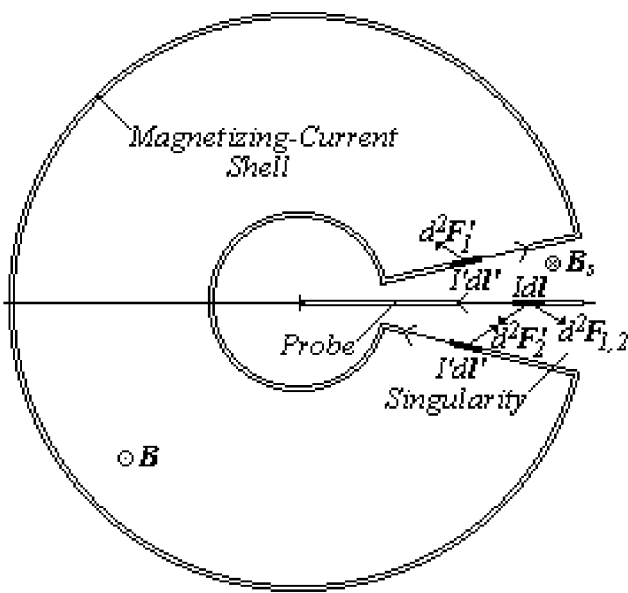
Figure 4: Magnetizing shell-probe Ampre interaction in the G-V dynamotor magnet singularity

conduction current through the probe and the equivalent magnetizing-shell current along the singularity's edges. While the upper-edge magnetizing current repels the probe with elementary forces $d^2\mathbf{F}_1$, the lower edge attracts the probe with forces $d^2\mathbf{F}_2$ resulting a high-magnitude clockwise torque on it.

3. Final Remarks

A conclusive statement on the superiority of the Ampre formulation for the analysis of the interaction beetween current-carrying wires and uniform magnets has been derived from the G-V experiments. The requirement of relative motion among both parts here, is in strict correspondence with the similar for generation action [10]. Conversely Grassmann SE -attributing motor action unilaterally to the probe wire even if attached to the magnet- fails in recognize homopolar machines' full symmetry.

The Ampre-formulation inclusion in electromagnetism programs at both intermediate and graduate levels seems a necessary outcome of this article.

This essay is ended with Maxwell's quote on the Ampre expression: *"The whole theory . . . is summed up in a formula . . . which must always remain the cardinal formula of electrodynamics"*. James Clerk Maxwell, *A Treatise on Electricity and Magnetism.* Dover (1954). [See also references 7 and 8].

"We are to admit no more causes of natural things than such as are both true and sufficient to explain their appearances." (Newton).

References

[1] J. Guala-Valverde & P. Mazzoni, *Apeiron*, **6**, 202 (1999).

[2] J. Guala-Valverde, P. Mazzoni, *Spacetime & Substance Journal*, **12**, N 4, 785 (1999).

[3] J. Guala Valverde, P. Mazzoni & R. Achilles, *American Journal of Physics*, **70**, N 10, 1052 (2002).

[4] J. Guala Valverde, *Physica Scripta.* **66**, 252, (2002).

[5] J. Guala-Valverde, *Spacetime & Substance*, **3**, 94 (2002)

[6] J. Guala-Valverde, "Infinite Energy." To be published (Dec. 2002)

[7] A.K.T. Assis, "Weber's Electrodynamics." Kluwer, Dordrecht, 1994.

[8] A.K.T. Assis, "Relational Mechanics." Apeiron, Montreal, 1999.

[9] K.K.H. Panofsky and M. Phillips, "Classical Electricity and Magnetism." Addisson Wesley, New York, 1955.

[10] T.E. Phipps Jr. & J. Guala-Valverde, *21st Century Science & Technology*, **11**, 55 (1998).

[11] M. Bueno & A.K.T. Assis, "Inductance and Force Calculation in Electrical Circuits." Nova Science Publishers, Huntinghton, New York, 2001.

Spacetime & Substance
Contents of issues for 2002 year

Vol. 3 (2002), No. 1 (11)

Vol. 3 (2002), No. 2 (12)

Vol. 3 (2002), No. 3 (13)

Vol. 3 (2002), No. 4 (14)

Vol. 3 (2002), No. 5 (15)

INFORMATION FOR AUTHORS

The Editorial Council accepts the manuscripts for the publication only in an electronic variant in the format for LATEX 2.09. They should be completely prepared for the publication. The manuscripts are accepted by e-mail or on diskettes (3.5"). The manuscripts can be adopted in other view only for familiarization.

The original manuscripts should be preferably no longer then 6 pages. They should contain no more than 4 figures. Length of the manuscript can be up to 10 pages only in exclusive cases (at arguing problems of primary importance). If the length of the manuscript exceeds 10 pages, it should be divided by the author into two or more papers, each of which should contain all pieces of a separate paper (title, authors, abstracts, text, references etc.). The Editorial Council accepts for the publication the brief reports too.

The payment for the publication of the manuscripts is not done. Each author gets the electronic version of that Journal edition, in which his paper was published free of charge.

An E-mail message acknowledging the receipt of the manuscript will be sent to the corresponding author within two working days after the manuscript receipt. If a message is not received please contact *krasnoh@iop.kiev.ua* to inquire about the manuscripts.

The Style File and Instructions for its use can be found at http://spacetime.narod.ru (sample.zip, 19 kb).

An abstract (within 20 lines) must be submitted. This one should be concise and complete regardless of the paper content. Include purpose, methodology, results, and conclusions. References should not be cited in the abstract. The abstract should be suitable for separate publication in an abstract journal and be adequate for indexing.

If the argument of an exponential is complicated or long, "exp" rather than "e" should be used. Awkward fractional composition can be avoided by the proper introduction of negative degrees. Solidus fractions (l/r) should be used, and enough enclosures should be included to avoid ambiguity in the text. According to the accepted convention, parentheses, brackets, and braces are in the order { [( )] }. Displayed equations should be numbered consecutively throughout the paper; the number (in parentheses) should be to the right of the equation.

Figures (black-and-while) should be of minimal size providing clear understanding. Breadth of the figure should not exceed 84 mm or 174 mm (in exclusive cases). Figures should be made out as separate files in the format of *.pcx (300 dpi/inch) or *.eps (minimum of kb).

Each figure must be cited in numerical order in the text and must have figure legend.

Tables should be typed as authors expect them to look in print. Every table must have a title, and all columns must have headings. Column headings must be arranged so that their relation to the data is clear. Footnotes should be indicated by reference marks [1], [2] etc. or by lowercase letters typed as superiors. Each table must be cited in the text.

The Editorial Council accepts also response on papers, published in the Journal. They should be no more than 1 journal page in length and should not contain figures but only to refer to the already published materials. But they can contain the formulas. The recalls are publishing in section "Discussion."

The list of references may be formed either by first citation in the text, or alphabetically.

Only works cited in the text should be included in the reference list. Personal communications and unpublished data or reports are not included in the reference list; they should be shown parenthetically in the text: (F.S. Jones, unpublished data, 1990).

The title of paper is permissible not to indicate. It is permissible to give only the initial page number of a paper. The format of the reference list is as indicated below.

References

[1] F.W. Stecker, K.J. Frost, *Nature*, **245**, 270 (1973).

[2] V.A. Brumberg, "Relativistic Celestial Mechanics", Nauka, Moskow, 1972 (in Russian).

[3] S.W. Hawking, in: "General Relativity. An Einstein Centenary Sutvey", eds. S.W. Hawking and W. Israel, *Cambr. Univ. Press*, Cambridge, England, 1979.

Read the Journal before sending a manuscript!

Spacetime & Substance

CONTENTS